FULL PAPER

Dalton
www.rsc.org/dalton

Alkene metatheses in transition metal coordination spheres: dimacrocyclizations that join *trans* positions of square-planar platinum complexes to give topologically novel diphosphine ligands

Takanori Shima, Eike B. Bauer, Frank Hampel and J. A. Gladysz*

Institut für Organische Chemie, Friedrich-Alexander-Universität Erlangen-Nürnberg, Henkestrasse 42, 91054 Erlangen, Germany

Received 6th January 2004, Accepted 11th February 2004
First published as an Advance Article on the web 24th February 2004

The alkene-containing phosphines $PPh((CH_2)_nCH{=}CH_2)_2$ (**4**) are prepared from $PPhH_2$, *n*-BuLi, and the corresponding bromoalkenes (1 : 2 : 2), and combined with the platinum tetrahydrothiophene complex $[Pt(\mu\text{-}Cl)(C_6F_5)(S(CH_2CH_2{-})_2)]_2$ (**12**) to give the square-planar adducts *trans*-$(Cl)(C_6F_5)Pt(PPh((CH_2)_nCH{=}CH_2)_2)_2$ (**11**, 93–73%; *n* = **a**, 2; **b**, 3; **c**, 4; **d**, 5; **e**, 6; **f**, 8). Ring-closing metatheses with Grubbs' catalyst (**2**) are studied. With **11e**, two isomers of *trans*-$(Cl)(C_6F_5)Pt(\overline{PPh(CH_2)_{14}P(CH_2)_{14}Ph})$ (**15e**) are isolated after hydrogenation. Both form *via* dimacrocyclization between the *trans*-phosphine ligands, but differ in the dispositions of the PPh rings (*syn*, 31%; *anti*, 7%). The alternative intraligand metathesis product *trans*-$(Cl)(C_6F_5)Pt(\overline{PPh(CH_2)_{14}})_2$ (**16e**) is independently prepared by (i) protecting **4e** as a borane adduct, $H_3B{\cdot}PPh((CH_2)_6CH{=}CH_2)_2$, (ii) cyclization with **2** and hydrogenation to give $H_3B{\cdot}\overline{PPh(CH_2)_{14}}$, (iii) deprotection and reaction with **12**. The sample derived from **11e** contains ≤2% **16e**; mass spectra suggest that the other products are dimers or oligomers. The structures of *syn*-**15e**, *anti*-**15e** and **16e** are verified crystallographically, and the macrocycle conformations analyzed. As expected from the $(CH_2)_n$ segment length, **11a** undergoes intraligand metathesis to give (*Z*,*Z*)-*trans*-$(Cl)(C_6F_5)Pt(\overline{PPh(CH_2)_2CH{=}CH(CH_2)_2})_2$ (86%), as confirmed by a crystal structure of the hydrogenation product. Although **11b** does not yield tractable products, **11c** gives *syn*-(*E*,*E*)-*trans*-$(Cl)(C_6F_5)Pt(\overline{PPh(CH_2)_4CH{=}CH(CH_2)_4P(CH_2)_4CH{=}CH(CH_2)_4Ph})$ (21%). This structure, and that of the hydrogenation product (*syn*-**15c**; 95%), are verified crystallographically. Analogous sequences with **11d**,**f** give *syn*-**15d**,**f** (5 and 14% overall).

Introduction

Alkene metathesis is seeing increasing use in syntheses of metal-containing molecules.[1] Among many applications, the generation of topologically novel metall*o*- and metall*a*macrocycles has attracted particular interest. This rapidly growing theme has its origins in Sauvage's elegant syntheses of catenanes,[2] and has been further developed by ourselves[3,4] and others.[5] In our previous full paper,[3d] we studied the series of square-planar sixteen-valence-electron platinum complexes *trans*-$(Cl)(C_6F_5)Pt(PPh_2(CH_2)_nCH{=}CH_2)_2$ (**1**) shown in Scheme 1. These feature monophosphine ligands with a polymethylene bridge to a terminal alkenyl group. Ring-closing metatheses with Grubbs' catalyst (**2**) gave high yields of thirteen to twenty-three membered macrocycles featuring unusual *trans*-spanning diphosphine ligands.[6] Mixtures of *E*/*Z* C=C isomers were obtained, but were easily hydrogenated to the saturated analogs **3**, which were robust and readily crystallized.

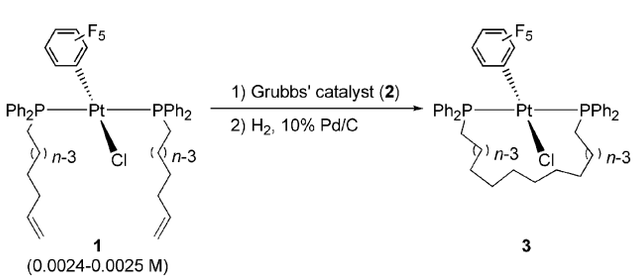

n	Yield, metathesis (%)[a]	Yield, hydrogenation (%)[b]	Overall yield (%)
4, **c**	95	70	67
6, **e**	96	72	69
8, **f**	90	59	53
9, **g**	85	50	43

[a] Includes minor amounts of dimeric or oligomeric byproducts.
[b] After chromatographic purification that removes dimeric or oligomeric byproducts.

Scheme 1 Monomacrocyclizations involving *trans* phosphine ligands with one alkene-containing substituent.

We established the feasibility of analogous reaction sequences with substituted polymethylene bridges[3d] and related square-planar rhodium complexes.[3c] However, we wondered whether this chemistry could be extended to topologically more complicated substrates. In particular, what might occur with similar complexes of phosphines containing *two* polymethylene bridges to terminal alkenyl groups – *e.g.*, $PPh((CH_2)_nCH{=}CH_2)_2$ (**4**)? As generalized in Scheme 2, two cyclization modes would be possible: (a) reaction between the *trans* phosphine ligands (interligand metathesis) to give an adduct of a macrocyclic *di*phosphine, also a metalladimacrocycle (**II**), or (b) reaction within the phosphine ligands (intraligand metathesis) to give a bis(adduct) of a cyclic monophosphine (**III**).

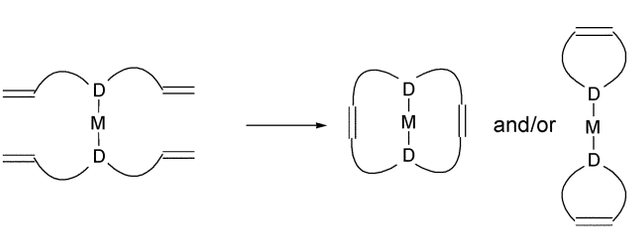

Scheme 2 Possible ring-closing metathesis modes for *trans* donor ligands with two alkene-containing substituents.

The feasibility of the second pathway had been explicitly demonstrated for the rhenium complexes **5h**,**i** shown in Scheme 3, which feature *one* ligand of the type **4** (*n* = 6). The

DOI: 10.1039/b400156g

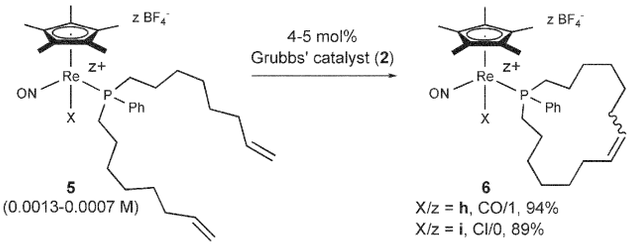

Scheme 3 Monomacrocyclizations involving phosphine ligands with two alkene-containing substituents.

metallomacrocycles **6h**,**i** could be isolated in 94–81% yields. The tungsten complex **7** in Scheme 4, which features *three* such ligands, is also relevant. It gave a complicated and nearly intractable mixture of all possible cyclization products (**8**, **9**, **10**), as established by mass spectrometric, HPLC, and crystallographic data. Although no attempt was made to vary the lengths of the $(CH_2)_n$ segments, it was evident that a simpler type of test substrate was needed. Accordingly, platinum complexes of **4**, *trans*-(Cl)(C_6F_5)Pt(PPh((CH$_2$)$_n$CH=CH$_2$)$_2$)$_2$ (**11**), were selected for intensive study.

In this paper, we describe the partitioning of **11** between the cyclization modes in Scheme 2 as a function of the number of methylene groups. Depending upon the chain length, either can dominate. However, dimeric or oligomeric species derived from intermolecular metathesis are generally the major products. Nonetheless, significant quantities of topologically novel diphosphine complexes of the type **II** can be accessed from several substrates. These would require lengthy syntheses *via* conventional methodologies. The crystal structures of four such compounds are determined, and their conformational features analyzed in detail. A small portion of this work has been communicated.[3b]

Results

1 Starting phosphines and complexes

As shown in eqn. (1), commercial $PPhH_2$ was successively treated at 0 °C with *n*-BuLi (2.0–2.1 equiv.) and then an α,ω-bromoalkene Br(CH$_2$)$_n$CH=CH$_2$ (*n* = **a**, 2; **b**, 3; **c**, 4; **d**, 5; **e**, 6; **f**, 8; 2.0–2.1 equiv.). Workups gave the requisite tertiary phosphines **4a**–**f** as colorless oils in 98–89% yields. The bromoalkenes were either commercially available or prepared from the corresponding alcohols as reported earlier.[3d] Other syntheses of **4a**,**b** have been published,[7,8] and the preparation of **4e** by this procedure has been described previously.[3c]

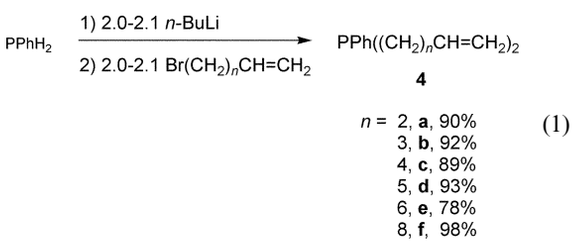

The phosphines **4a**–**f** were combined with the platinum tetrahydrothiophene complex [Pt(μ-Cl)(C_6F_5)(S(CH$_2$CH$_2$–)$_2$)]$_2$ (**12**)[9] under conditions used to prepare the educts **1** in Scheme 1 earlier.[10] As shown in Scheme 5, workups gave the bis(phosphine) complexes **11a**–**f** as colorless oils in 93–73% yields. The new phosphines and platinum complexes were characterized by NMR (^{1}H, ^{13}C, ^{31}P) and IR spectroscopy, mass spectrometry, and microanalyses, as summarized in the experimental section. The spectroscopic properties of **11a**–**f** were similar to those of the educts in Scheme 1 and related triarylphosphine complexes reported previously.[11]

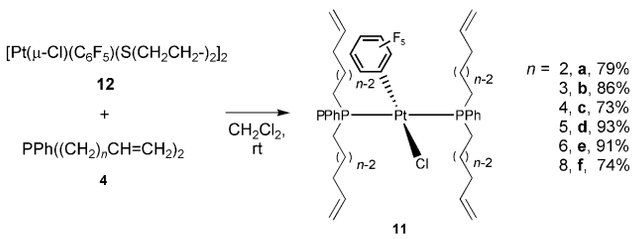

Scheme 5 Synthesis of substrates for alkene metatheses.

2 Ring-closing metathesis of 11e

Alkene metatheses were conducted under conditions similar to those used in Scheme 1. As shown in Scheme 6, **11e** (*ca*. 0.0034 M) and **2** (10 mol%, added in two portions) were reacted in refluxing CH_2Cl_2. Although the catalyst loading might appear somewhat high, it should be divided by two to normalize to the number of ring closures. The mixture was filtered through alumina to separate the catalyst residue. The metathesis products, for which **13e** and **14e** are the only possible monomeric structures, were obtained in 97% yield. The sample was characterized as described for **11a**–**f**.

The ^{1}H NMR spectrum showed no terminal alkene residues, indicating metathesis to be ≥98% complete. Accordingly, new CH=CH signals were detected between 5.20 and 5.35 ppm, presumably due to both *E* and *Z* isomers. The ^{31}P NMR spectrum exhibited a multitude of peaks, the dominant one of which represented 44% of the total area. The ^{13}C NMR spectrum exhibited an even more complex mixture of peaks. These were not tabulated, but only signals in the aromatic/alkene (132–126.5 ppm) and aliphatic (32.8–23.0 ppm) regions were observed.

The microanalysis fit the formulae of **13e**, **14e**, or related species derived from intermolecular metathesis. The mass spectrum showed a significant ion with a mass corresponding to [**13e** − Cl]$^+$ or [**14e** − Cl]$^+$ (*m*/*z* 966, 45% relative intensity). Another ion had the formal composition [2·**13e** − Cl]$^+$ or [2·**14e** − Cl]$^+$ (*m*/*z* 1969, 30%), indicating the presence of dimeric or oligomeric byproducts. Analogous ions were *not* observed for the macrocyclizations in Scheme 1. In order to simplify further analysis and product isolation, a hydrogenation was conducted.

The metathesis mixture was treated with H_2 (1 atm) in the presence of 10% Pd/C (Scheme 6). Filtration through alumina

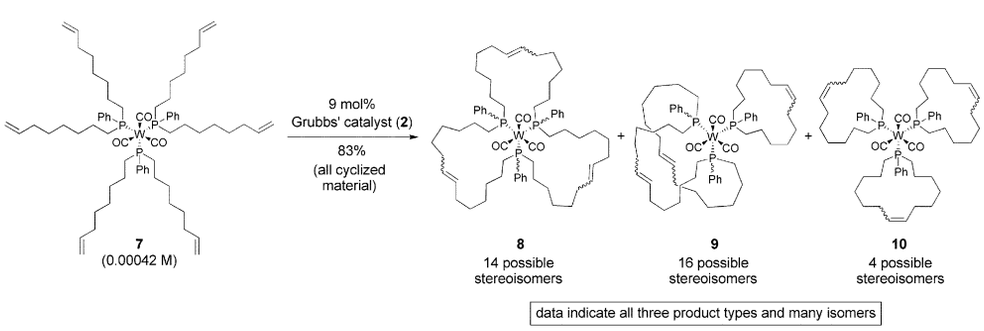

Scheme 4 Polymacrocyclizations involving phosphine ligands with two alkene-containing substituents.

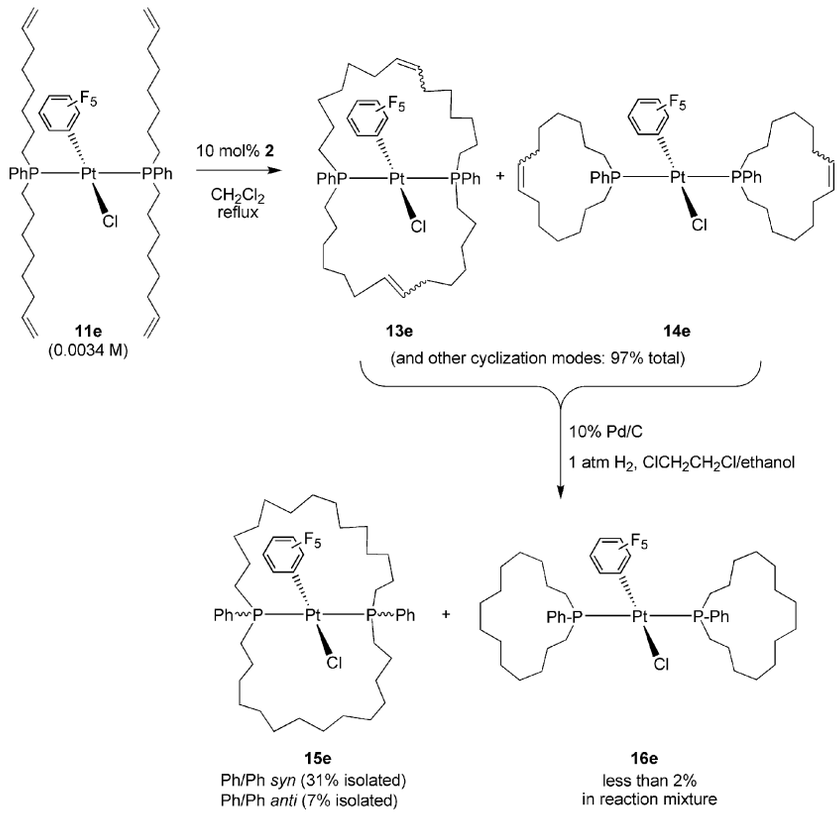

Scheme 6 Ring-closing metathesis/hydrogenation sequence for **11e**.

gave the crude saturated macrocycles (77%), for which **15e** and **16e** are the only possible monomeric structures. The ^{1}H NMR spectrum showed that all double bonds had been reduced, but the ^{31}P NMR spectrum still exhibited many signals. The dominant peak represented 52% of the total area, and matched the chemical shift of *syn*-**15e** (see below). The mass spectrum showed significant ions with masses corresponding to **15e**$^{+}$ or **16e**$^{+}$ (*m*/*z* 1006, 40%) and [**15e** − Cl]$^{+}$ or [**16e** − Cl]$^{+}$ (*m*/*z* 970, 100%). Diplatinum ions of the formal composition [2·**15e** − Cl]$^{+}$ or [2·**16e** − Cl]$^{+}$ (*m*/*z* 1977, 20%) were also evident.

The sample was chromatographed on alumina. The two least polar products were isolated as white powders in 31 and 7% yields, and characterized analogously to **11a**–**f**. The mass spectra indicated that both were monoplatinum species. The first product exhibited a single ^{31}P NMR signal, and seven methylene ^{13}C NMR signals, whereas the second exhibited two mutually coupled ^{31}P NMR signals and several additional methylene ^{13}C NMR signals. Complexes of the type **15e** can exist as two stereoisomers, differing in the relative orientations of the phenyl groups (*syn* or *anti*). Accordingly, crystal structures described below showed the products to be *syn*-**15e** and *anti*-**15e**, respectively. The contrasting NMR properties are further analyzed below.

3 Independent synthesis of an intraligand metathesis product

We wanted to be certain that the workups in Scheme 6 did not overlook products derived from intraligand metathesis (**14e**, **16e**). Thus, an independent synthesis was sought. An initial ring-closing metathesis of the free phosphine **4e** was considered. However, Grubbs' catalyst **2** is not normally effective with alkenes that contain phosphines,[12] and there are only scattered successes with Schrock-type catalysts.[12b,13] In contrast, phosphines in which the lone pairs are protected with borane are reliable substrates for alkene metatheses.[12] Hence, the sequence summarized in Scheme 7 was investigated.

A potential problem was obvious at the outset. Reactions of alkene-containing phosphines with borane sources can lead either to protected phosphines or alkene hydroboration. In some cases, the latter event can be circumvented by introducing the alkene moieties subsequent to phosphorus protection.[12a] Fortunately, the reaction of $H_3B{\cdot}SMe_2$ and **4e** at −20 °C gave the target compound **17e** in 65% yield. The ^{31}P NMR spectrum showed coupling to boron ($^{1}J(^{31}P,^{11}B)$ 75 Hz), and the ^{1}H NMR spectrum exhibited a broad BH_3 signal (1.0–0.2 ppm).

As illustrated in Scheme 7, ring-closing metathesis of **17e** with **2** gave the crude 15-membered cyclic phosphine derivative **18e** in 62–91% yields. Unlike the monomacrocyclizations in Scheme 1, the mass spectrum exhibited ions corresponding both to intramolecular and intermolecular metathesis products (**18e**$^{+}$, *m*/*z* 315, 80%; formal composition [2·**18e**]$^{+}$, *m*/*z* 629, 20%). The ^{1}H NMR spectrum showed three closely spaced multiplets in the C*H*=C*H* region (*ca.* 1 : 1 : 1), consistent with a mixture of *E*/*Z* isomers and/or intra/intermolecular products.

When **18e** was subjected to the hydrogenation conditions in Schemes 1 and 6 (10% Pd/C, 1 atm H_2), as well as higher H_2 pressures (6 atm), no reaction occurred. Thus, **18e** and H_2 (6 atm) were combined in the presence of Wilkinson's catalyst. Chromatography gave the saturated cyclic phosphine derivative **19e** in 77–74% yields. The ^{31}P NMR spectrum showed one signal ($^{1}J(^{31}P,^{11}B)$ 70 Hz), and the ^{13}C NMR spectrum was much simpler than that of **19e**. However, besides the seven expected methylene signals, several minor peaks were evident (<10%). The mass spectrum also showed, in addition to ions derived from **19e**, some diphosphorus species. Hence, the chromatography conditions did not completely remove the material derived from intermolecular metathesis.

As shown in Scheme 7, **19e** was deprotected by a standard procedure using $HNEt_2$.[14] The crude cyclic phosphine $\overline{PPh(CH_2)_{14}}$ (**20e**) was directly reacted with the tetrahydrothiophene complex **12**. Chromatography gave the target complex **16e** in 24% overall yield from **19e**. The mass spectrum exhibited only monoplatinum ions. The most intense peaks involved phosphine ligand loss, in contrast to *syn*-**15e** and *anti*-**15e** where no such fragments were observed. NMR spectra showed no traces of any byproducts. The ^{31}P signal (7.2 ppm)

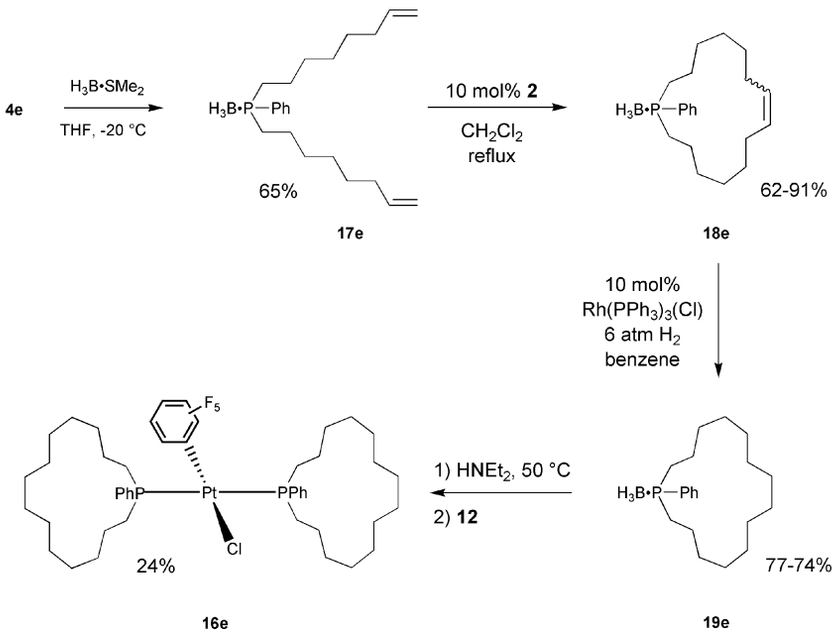

Scheme 7 Synthesis of an authentic sample of **16e**.

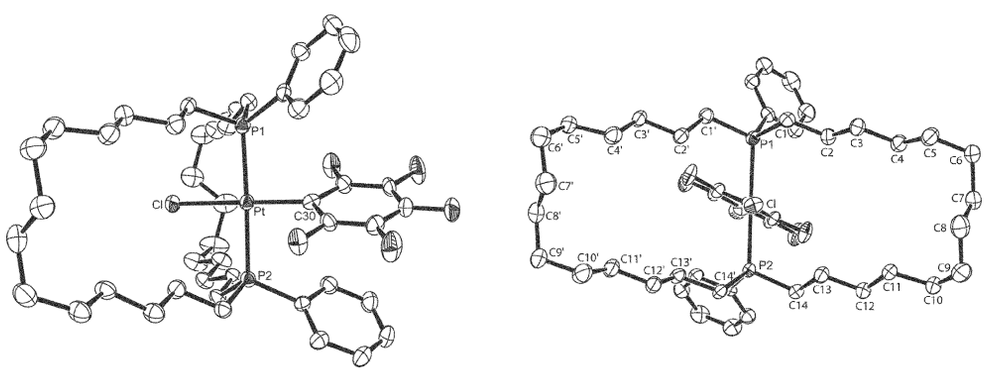

Fig. 1 Molecular structure of *syn*-**15e**.

was considerably upfield from those of *syn*-**15e** (11.8 ppm) and *anti*-**15e** (15.8, 11.2 ppm).

The ^{31}P NMR spectrum of the crude hydrogenation product in Scheme 6 was reinvestigated. A small peak with a chemical shift close to that of **16e** was apparent. Integration allowed an upper limit of 2% to be placed upon the yield of **16e** from **11e**. The NMR tube was doped with a small amount of the independently synthesized **16e** to confirm that the chemical shifts were identical. Finally, *syn*-**15e**, *anti*-**15e**, and **16e** were compared by alumina TLC (1 : 3 v/v CH_2Cl_2–hexanes). R_f values of 0.56, 0.44, and 0.20 were found. Those of the various byproducts from Scheme 6 were much lower.

4 Structural and dynamic properties of *syn*-15e, *anti*-15e and 16e

The crystal structures of *syn*-**15e** and *anti*-**15e** were determined as summarized in Table 1 and the experimental section. Key bond lengths, bond angles, and torsion angles are listed in Table 2.[15] The two macrocycles in each compound are given primed and unprimed atom labels so that their features are more easily compared. The molecular structure of *syn*-**15e** is depicted in Fig. 1 and that of *anti*-**15e** in Fig. 2. The left views in Figs. 1 and 2 highlight the contrasting orientations of the phenyl rings with respect to the platinum square planes. The isomers also exhibit markedly different macrocycle conformations.

A $C_6H_5/C_6F_5/C_6H_5$ π stacking interaction is evident in *syn*-**15e** (Fig. 1). This feature is also found in the crystal structures of **3c**,**e**–**g**, (Scheme 1).[3d] It is now well established that C_6H_5/C_6F_5 π interactions are attractive and a driving force in many crystallizations.[16] The average of the two centroid–centroid distances in *syn*-**15e** is 4.05 Å. This is somewhat greater than in **3e** (3.60 Å), the related complex with only one $P(CH_2)_{14}P$ bridge. In contrast, *anti*-**15e** exhibits a single C_6H_5/C_6F_5 π interaction (Fig. 2). It is not as pronounced, with a centroid–centroid distance of 4.26 Å.

The crystal structure of **16e** was similarly determined. Views that highlight the *trans* relationship of the macrocyclic monophosphine ligands are given in Fig. 3. Selected metrical parameters are listed in Table 3. Like *anti*-**15e**, **16e** exhibits a single, somewhat weak C_6H_5/C_6F_5 π interaction, with a centroid–centroid distance of 4.49 Å.

The symmetry properties of *syn*-**15e** and *anti*-**15e** are relevant to several observations. As illustrated in Fig. 4, *syn*-**15e** has idealized C_{2v} symmetry. The phosphorus atoms and phenyl rings are homotopic; they can be exchanged by a rotation around the Cl–Pt–C_6F_5 axis. Each carbon atom of a given macrocycle has a homotopic counterpart in the other macrocycle. In addition, the carbon atoms labeled C_a in Fig. 4 are enantiotopic with the carbon atoms labeled C_b. However, the geminal protons of each methylene group are diastereotopic.

In contrast, *anti*-**15e** has C_1 symmetry. As illustrated in Fig. 4, both phosphorus atoms and phenyl rings are diastereotopic. The same holds for all carbon atoms of the macrocycles, as well as the geminal protons of the methylene groups. Hence, the NMR spectra of *anti*-**15e** should be more complicated than those of *syn*-**15e**, in accord with observations above and additional details provided in the experimental section. For example, the ^{31}P NMR spectrum of *anti*-**15e** shows an AB spin system, with distinct $^1J_{PtP}$ values for each signal.

Table 1 General crystallographic data[a]

Complex	*syn*-(*E*,*E*)-**13c**	*syn*-**15c**	*syn*-**15e**	*anti*-**15e**	**16a**	**16e**
Formula	$C_{38}H_{46}ClF_5P_2Pt$	$C_{38}H_{50}ClF_5P_2Pt$	$C_{46}H_{66}ClF_5P_2Pt$	$C_{46}H_{66}ClF_5P_2Pt$	$C_{30}H_{34}ClF_5P_2Pt$	$C_{46}H_{66}ClF_5P_2Pt$
Formula weight	890.23	894.26	1006.47	1006.47	782.05	1006.47
Crystal system	Monoclinic	Monoclinic	Monoclinic	Triclinic	Orthorhombic	Triclinic
Space group	$P2_1/n$	$P2_1/c$	$P2_1/c$	$P\bar{1}$	*Pbcn*	$P\bar{1}$
a/Å	13.64790(10)	23.5432(11)	24.8121(3)	11.69470(10)	18.5572(3)	10.57500(10)
b/Å	19.0165(3)	15.7182(6)	10.5438(2)	13.29450(10)	10.9033(2)	12.2670(2)
c/Å	15.0138(2)	21.5805(6)	18.0730(4)	14.9666(2)	28.7856(5)	18.1630(3)
α/°	90	90	90	88.3340(10)	90	72.9290(9)
β/°	106.7190(10)	112.273(2)	104.6070(10)	81.1850(10)	90	84.6100(8)
γ/°	90	90	90	76.1950(10)	90	82.4310(8)
V/Å^3	3731.89(8)	7390.2(5)	4575.32(14)	2232.96(4)	5824.33(17)	2228.93(6)
Z	4	8	4	2	8	2
D_c/Mg m^{-3}	1.584	1.607	1.461	1.495	1.784	1.500
μ/mm^{-1}	3.968	4.008	3.246	3.325	5.071	3.331
F(000)	1776	3584	2048	1022	3072	1024
Crystal size/mm	0.35 × 0.20 × 0.20	0.10 × 0.10 × 0.10	0.30 × 0.20 × 0.10	0.1 × 0.1 × 0.1	0.30 × 0.20 × 0.20	0.20 × 0.20 × 0.10
θ Limit/°	1.89–27.48	1.60–25.02	2.11–27.51	1.38–25.05	1.41–27.48	2.21–27.52
Index ranges *hkl*	−17 to 17, −24 to 24, −19 to 19	−27 to 28, −18 to 18, −24 to 25	−31 to 32, −12 to 13, −23 to 23	−13 to 13, −15 to 15, −17 to 17	−24 to 24, −14 to 14, −37 to 37	−13 to 13, −15 to 15, −23 to 23
Reflections collected	16508	43886	17699	15379	12286	19533
Independent reflections	8549	13024	10322	7900	6642	10238
Reflections [$I > 2\sigma(I)$]	7851	6875	7022	7011	5538	9428
Data/restraints/parameters	8549/0/424	13024/0/847	10322/0/496	7900/0/496	6642/0/352	10238/0/496
Goodness-of-fit on F^2	1.061	0.930	0.998	1.152	1.116	1.029
Final *R* indices [$I > 2\sigma(I)$]	$R1 = 0.0199$, $wR2 = 0.0491$	$R1 = 0.0449$, $wR2 = 0.0958$	$R1 = 0.0404$, $wR2 = 0.0695$	$R1 = 0.0247$, $wR2 = 0.0601$	$R1 = 0.0240$, $wR2 = 0.0602$	$R1 = 0.0268$, $wR2 = 0.0621$
R Indices (all data)	$R1 = 0.0233$, $wR2 = 0.0505$	$R1 = 0.1156$, $wR2 = 0.1319$	$R1 = 0.0860$, $wR2 = 0.0796$	$R1 = 0.0324$, $wR2 = 0.0751$	$R1 = 0.0334$, $wR2 = 0.0751$	$R1 = 0.0305$, $wR2 = 0.0636$
Largest diff. peak and hole $\Delta\rho$/e Å^{-3}	0.997 and −0.966	0.894 and −1.307	2.621 and −1.408	1.371 and −0.978	0.893 and −0.996	1.431 and −0.920

[a] Data common to all structures: diffractometer, Nonius Kappa CCD; wavelength, 0.71073 Å; temperature, 173(2) K.

Table 2 Key bond lengths, bond angles, and torsion angles for interligand metathesis products

Complex	*syn*-(*E*,*E*)-**13c**	*syn*-**15c**		*syn*-**15e**	*anti*-**15e**
		First molecule[a]	Second molecule[a]		
Bond lengths (Å)					
Pt–P(1)/Pt–P(2)	2.3064(6)/2.2984(6)	2.313(2)/2.303(2)	2.323(2)/2.318(3)	2.3139(11)/2.3075(11)	2.2970(10)/2.2986(9)
Pt–Cl	2.3671(5)	2.377(2)	2.380(3)	2.3778(11)	2.3560(10)
Pt–C(30)	2.015(2)	1.989(10)	2.005(11)	2.002(4)	2.017(4)
C(1)–C(2)/C(1′)–C(2′)	1.531(3)/1.533(3)	1.526(14)/1.522(14)	1.529(13)/1.520(17)	1.515(6)/1.540(5)	1.522(6)/1.522(5)
C(2)–C(3)/C(2′)–C(3′)	1.523(3)/1.528(3)	1.532(14)/1.569(18)	1.517(13)/1.533(17)	1.518(6)/1.514(6)	1.533(7)/1.532(6)
C(3)–C(4)/C(3′)–C(4′)	1.530(3)/1.530(4)	1.508(15)/1.345(19)	1.491(14)/1.536(18)	1.518(6)/1.504(6)	1.503(8)/1.513(7)
C(4)–C(5)/C(4′)–C(5′)	1.493(4)/1.502(4)	1.505(14)/1.471(16)	1.558(15)/1.497(17)	1.520(6)/1.516(6)	1.508(7)/1.520(6)
C(5)–C(6)/C(5′)–C(6′)	1.316(4)/1.314(4)	1.523(13)/1.526(16)	1.430(17)/1.513(17)	1.518(7)/1.521(6)	1.519(8)/1.522(7)
C(6)–C(7)/C(6′)–C(7′)	1.492(4)/1.502(4)	1.502(13)/1.490(15)	1.565(15)/1.506(15)	1.509(7)/1.534(6)	1.489(8)/1.513(6)
C(7)–C(8)/C(7′)–C(8′)	1.526(4)/1.529(4)	1.525(15)/1.509(16)	1.470(16)/1.494(15)	1.515(7)/1.505(7)	1.530(8)/1.525(6)
C(8)–C(9)/C(8′)–C(9′)	1.525(3)/1.521(3)	1.504(14)/1.456(16)	1.549(14)/1.497(15)	1.547(6)/1.545(7)	1.548(7)/1.521(6)
C(9)–C(10)/C(9′)–C(10′)	1.524(3)/1.530(3)	1.533(14)/1.500(15)	1.515(15)/1.484(16)	1.515(6)/1.531(7)	1.524(7)/1.523(6)
C(10)–C(11)/C(10′)–C(11′)	–	–	–	1.520(6)/1.508(6)	1.509(7)/1.513(6)
C(11)–C(12)/C(11′)–C(12′)	–	–	–	1.518(6)/1.508(6)	1.511(7)/1.515(6)
C(12)–C(13)/C(12′)–C(13′)	–	–	–	1.513(6)/1.528(6)	1.521(6)/1.517(6)
C(13)–C(14)/C(13′)–C(14′)	–	–	–	1.526(6)/1.525(6)	1.527(6)/1.529(5)
Bond angles (°)					
C(30)–Pt–P(1)	94.00(6)	94.6(3)	89.4(3)	90.47(12)	93.31(10)
C(30)–Pt–P(2)	91.50(6)	91.3(3)	93.1(3)	91.51(12)	87.42(10)
P(1)–Pt–P(2)	174.41(2)	172.21(10)	173.96(11)	177.99(4)	173.33(3)
C(30)–Pt–Cl	178.06(6)	178.3(3)	179.3(3)	178.89(13)	175.18(11)
P(1)–Pt–Cl	84.062(19)	86.83(9)	90.42(10)	88.89(4)	86.71(3)
P(2)–Pt–Cl	90.44(2)	87.37(9)	86.94(9)	89.14(4)	93.12(3)
Torsion angles (°)					
P(2)–Pt–P(1)–C(1)/P(2)–Pt–P(1)–C(1′)	45.2(2)/–70.5(2)	19.8(9)/–95.2(8)	−22.4(11)/–139.9(10)	−69.1(12)/49.8(12)	90.3(3)/–145.5(3)
Pt–P(1)–C(1)–C(2)/Pt–P(1)–C(1′)–C(2′)	35.56(19)/–50.42(19)	59.0(8)/–70.8(9)	47.8(9)/51.5(11)	46.5(4)/56.5(3)	−160.1(3)/–44.7(3)
P(1)–C(1)–C(2)–C(3)/P(1)–C(1′)–C(2′)–C(3′)	−176.85(17)/179.15(18)	176.6(7)/69.1(12)	−157.9(8)/–94.5(13)	−175.3(3)/–164.6(3)	172.5(3)/161.9(3)
C(1)–C(2)–C(3)–C(4)/C(1′)–C(2′)–C(3′)–C(4′)	172.4(2)/–75.0(3)	60.8(12)/156.7(16)	179.6(9)/172.6(11)	178.8(4)/–180.0(4)	−54.1(5)/−174.3(3)
C(2)–C(3)–C(4)–C(5)/C(2′)–C(3′)–C(4′)–C(5′)	−64.2(3)/–67.6(3)	53.5(13)/174.3(13)	−67.6(14)/172.8(12)	−176.7(4)/–177.4(4)	−59.0(5)/60.7(5)
C(3)–C(4)–C(5)–C(6)/C(3′)–C(4′)–C(5′)–C(6′)	131.5(3)/129.7(3)	52.8(14)/83.8(19)	107.7(13)/45.1(16)	−170.2(4)/–176.5(4)	178.1(4)/56.0(5)
C(4)–C(5)–C(6)–C(7)/C(4′)–C(5′)–C(6′)–C(7′)	−175.2(2)/179.4(2)	170.5(9)/–157.9(13)	177.0(10)/60.4(15)	−51.7(6)/–60.6(7)	179.6(4)/169.1(4)
C(5)–C(6)–C(7)–C(8)/C(5′)–C(6′)–C(7′)–C(8′)	118.4(3)/132.5(3)	56.0(13)/97.0(14)	59.4(15)/–169.9(11)	−62.1(6)/–67.0(7)	71.5(6)/–175.8(4)
C(6)–C(7)–C(8)–C(9)/C(6′)–C(7′)–C(8′)–C(9′)	−66.7(3)/–68.5(3)	53.6(14)/–58.9(15)	57.9(15)/–166.1(11)	−179.6(4)/–176.7(4)	75.9(6)/–179.1(4)
C(7)–C(8)–C(9)–C(10)/C(7′)–C(8′)–C(9′)–C(10′)	179.6(2)/166.0(2)	−179.1(8)/176.0(11)	−174.7(10)/–61.8(15)	−61.9(6)/–60.5(7)	−167.7(4)/72.4(5)
C(8)–C(9)–C(10)–C(11)/C(8′)–C(9′)–C(10′)–C(11′)	–	–	–	−59.7(6)/–50.4(7)	−173.7(4)/72.9(5)
C(9)–C(10)–C(11)–C(12)/C(9′)–C(10′)–C(11′)–C(12′)	–	–	–	−178.6(4)/–171.3(4)	−167.2(4)/–177.4(3)
C(10)–C(11)–C(12)–C(13)/C(10′)–C(11′)–C(12′)–C(13′)	–	–	–	176.3(4)/–170.4(4)	73.8(5)/62.0(5)
C(11)–C(12)–C(13)–C(14)/C(11′)–C(12′)–C(13′)–C(14′)	–	–	–	−179.1(4)/–174.0(4)	75.0(5)/51.8(5)
C(n − 2)–C(n − 1)–C(n)–P(2)/C(n' − 2)–C(n' − 1)–C(n')–P(2)[b]	175.99(19)/–163.28(17)	154.6(7)/–168.0(9)	169.8(7)/–69.7(13)	−169.7(3)/–172.2(3)	177.4(3)/–179.7(3)
C(n − 1)–C(n)–P(2)–Pt/C(n' − 1)–C(n')–P(2)–Pt[b]	42.9(2)/53.70(18)	−44.2(8)/36.9(11)	−48.2(9)/82.7(9)	56.0(4)/39.2(4)	53.6(3)/167.6(3)
C(n)–P(2)–Pt–P(1)/C(n')–P(2)–Pt–P(1)[b]	−74.4(2)/43.0(2)	−11.6(9)/102.2(8)	8.6(12)/121.2(10)	28.1(12)/−91.9(12)	−23.4(3)/96.9(3)

[a] Independent molecules in the unit cell. [b] n = Number of carbons in macrocycle.

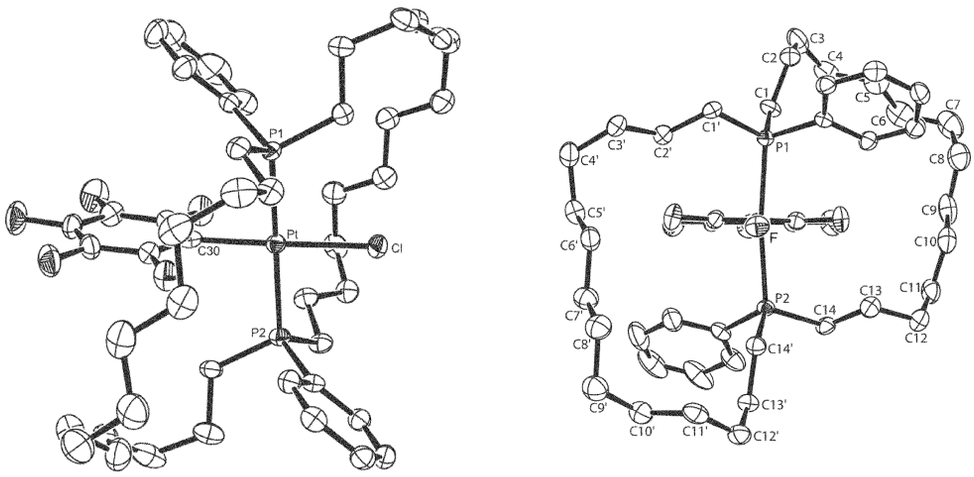

Fig. 2 Molecular structure of *anti*-**15e**.

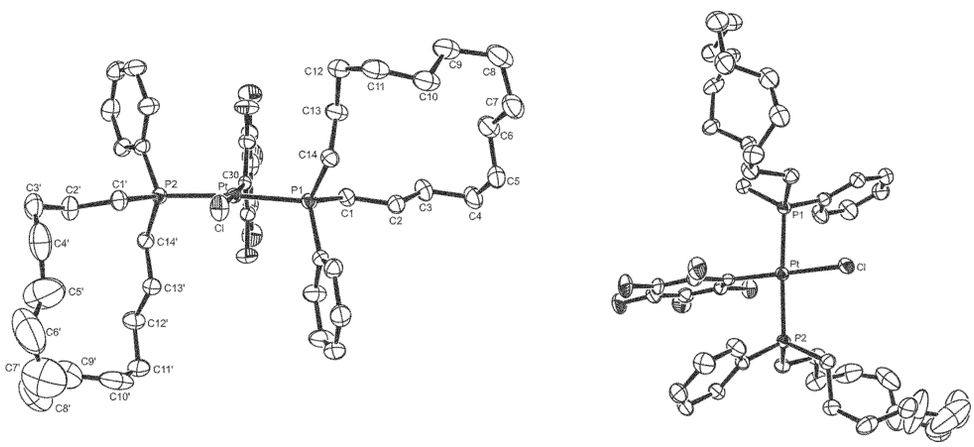

Fig. 3 Molecular structure of **16e**.

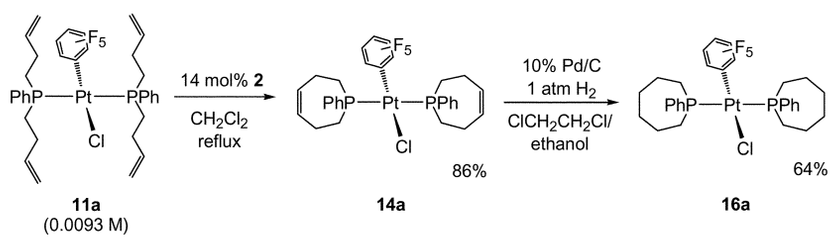

Scheme 8 Ring-closing metathesis/hydrogenation sequence for **11a**.

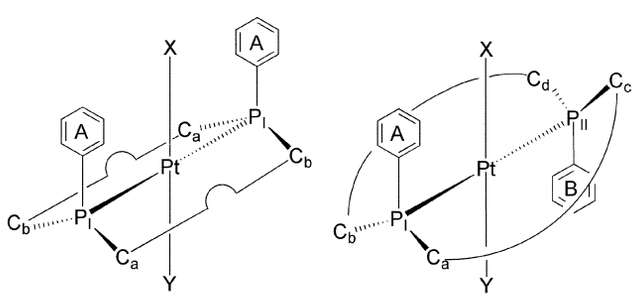

IV
(*syn*-**15**)
C_{2v}
homotopic:
P_I/P_I, Ph_A/Ph_A, C_a/C_a, C_b/C_b
enantiotopic:
C_a/C_b

V
(*anti*-**15**)
C_1
diastereotopic:
P_I/P_{II}, Ph_A/Ph_B, $C_a/C_b/C_c/C_d$

Fig. 4 Idealized structures and stereochemical relationships in **15**.

A toluene-d_8 solution of *anti*-**15e** was warmed to 95 °C while ^{31}P NMR spectra were periodically recorded. No coalescence or significant broadening of the ^{31}P NMR signals was noted, and no new peaks derived from *syn*-**15e** or other species appeared. Application of the coalescence formula,[17] using the $\Delta\nu$ and J values for the phosphorus atoms from the low temperature limit (618.2 and 426.8 Hz, 25 °C), allowed a lower limit of 16.4 kcal mol^{-1} (95 °C) to be placed on any process capable of rendering the phosphorus atoms of *anti*-**15e** equivalent. One such possibility, which should become accessible with longer $P(CH_2)_nP$ bridges, is analyzed in the discussion section.

5 Ring-closing metatheses of 11a,b,c,d,f

Complex **11a**, which features short $(CH_2)_2$ segments between the phosphorus and terminal alkenyl moieties, would be a very unlikely candidate for interligand metathesis, or cyclization mode **II** in Scheme 2. The *trans* phosphorus atoms would be bridged by only six carbon atoms, resulting in a highly strained nine-membered ring. The shortest known saturated bridge between *trans* phosphorus atoms in a square planar complex consists of nine methylene groups, giving a twelve-membered ring.[6,18]

As shown in Scheme 8, **11a** (0.0093 M) and **2** were combined under conditions analogous to those in Schemes 1 and 6. Workup gave the expected intraligand metathesis product, bis(monophosphine) complex (*Z*,*Z*)-**14a**, in 86% yield.

Table 3 Key bond lengths, bond angles, and torsion angles for intraligand metathesis products

Complex	**16a**	**16e**
Bond lengths (Å)		
Pt–P(1)/Pt–P(2)	2.3129(9)/2.3056(9)	2.2972(7)/2.3049(7)
Pt–Cl	2.3660(8)	2.3554(7)
Pt–C(30)	2.017(3)	2.017(3)
C(1)–C(2)/C(1′)–C(2′)	1.527(6)/1.537(5)	1.535(4)/1.533(4)
C(2)–C(3)/C(2′)–C(3′)	1.510(7)/1.516(6)	1.520(4)/1.515(5)
C(3)–C(4)/C(3′)–C(4′)	1.513(7)/1.533(6)	1.530(5)/1.512(6)
C(4)–C(5)/C(4′)–C(5′)	1.523(5)/1.527(6)	1.519(5)/1.564(9)
C(5)–C(6)/C(5′)–C(6′)	1.540(5)/1.530(5)	1.524(5)/1.291(11)[b]
C(6)–C(7)/C(6′)–C(7′)	–	1.522(5)/1.428(11)[b]
C(7)–C(8)/C(7′)–C(8′)	–	1.517(6)/1.388(9)[b]
C(8)–C(9)/C(8′)–C(9′)	–	1.562(6)/1.578(8)
C(9)–C(10)/C(9′)–C(10′)	–	1.504(5)/1.487(7)
C(10)–C(11)/C(10′)–C(11′)	–	1.513(6)/1.554(8)
C(11)–C(12)/C(11′)–C(12′)	–	1.503(5)/1.531(6)
C(12)–C(13)/C(12′)–C(13′)	–	1.528(5)/1.524(5)
C(13)–C(14)/C(13′)–C(14′)	–	1.541(4)/1.532(4)
Bond angles (°)		
C(30)–Pt–P(1)/C(30)–Pt–P(2)	91.23(9)/93.41(9)	93.69(7)/87.72(7)
P(1)–Pt–P(2)	174.84(3)	175.54(3)
C(30)–Pt–Cl	177.99(10)	177.52(8)
P(1)–Pt–Cl/P(2)–Pt–Cl	86.85(3)/88.53(3)	86.39(3)/92.38(3)
Torsion angles (°)		
P(2)–Pt–P(1)–C(1)/P(1)–Pt–P(2)–C(1′)	32.9(4)/–170.9(4)	−104.1(3)/77.9(3)
Pt–P(1)–C(1)–C(2)/Pt–P(2)–C(1′)–C(2′)	−152.5(3)/–49.7(3)	−176.24(18)/–170.6(2)
P(1)–C(1)–C(2)–C(3)/P(2)–C(1′)–C(2′)–C(3′)	63.4(5)/–33.1(4)	−166.7(2)/–173.1(3)
C(1)–C(2)–C(3)–C(4)/C(1′)–C(2′)–C(3′)–C(4′)	−94.9(5)/–49.2(5)	−177.8(3)/–57.8(5)
C(2)–C(3)–C(4)–C(5)/C(2′)–C(3′)–C(4′)–C(5′)	39.1(5)/94.8(4)	−54.3(4)/–55.5(5)
C(3)–C(4)–C(5)–C(6)/C(3′)–C(4′)–C(5′)–C(6′)	50.0(5)/–72.3(4)	−54.9(4)/–148.0(9)
C(4)–C(5)–C(6)–C(7)/C(4′)–C(5′)–C(6′)–C(7′)	–	178.3(3)/–162.0(2)
C(5)–C(6)–C(7)–C(8)/C(5′)–C(6′)–C(7′)–C(8′)	–	−169.2(3)/–60.6(14)
C(6)–C(7)–C(8)–C(9)/C(6′)–C(7′)–C(8′)–C(9′)	–	60.5(5)/77.8(11)
C(7)–C(8)–C(9)–C(10)/C(7′)–C(8′)–C(9′)–C(10′)	–	52.3(5)/56.7(9)
C(8)–C(9)–C(10)–C(11)/C(8′)–C(9′)–C(10′)–C(11′)	–	170.6(3)/171.8(5)
C(9)–C(10)–C(11)–C(12)/C(9′)–C(10′)–C(11′)–C(12′)	–	57.5(4)/61.9(5)
C(10)–C(11)–C(12)–C(13)/C(10′)–C(11′)–C(12′)–C(13′)	–	53.5(5)/58.1(5)
C(11)–C(12)–C(13)–C(14)/C(11′)–C(12′)–C(13′)–C(14′)	–	52.9(4)/–179.9(3)
C(*n* − 2)–C(*n* − 1)–C(*n*)–P(1)/C(*n* − 2′)–C(*n* − 1′)–C(*n*′)–P(2)[a]	−92.7(4)/59.1(4)	161.3(2)/171.4(2)
C(*n* − 1)–C(*n*)–P(1)–C(1)/C(*n* − 1′)–C(*n*′)–P(2)–C(1′)[a]	54.1(3)/–70.6(3)	50.3(2)/–46.1(3)
C(*n*)–P(1)–C(1)–C(2)/C(*n*′)–P(2)–C(1′)–C(2′)[a]	−30.9(4)/79.2(3)	57.0(3)/–63.1(2)
Pt–P(1)–C(*n*)–C(*n* − 1)/Pt–P(2)–C(*n*′)–C(*n* − 1′)[a]	174.5(2)/61.5(3)	−79.9(2)/63.0(2)
P(2)–Pt–P(1)–C(*n*)/P(1)–Pt–P(2)–C(*n*′)[a]	−86.4(4)/65.5(4)	−133.0(3)/–42.3(4)

[a] *n* = Number of methylene groups in macrocycle. [b] The thermal ellipsoids for C(5′) to C(8′) are very elongated.

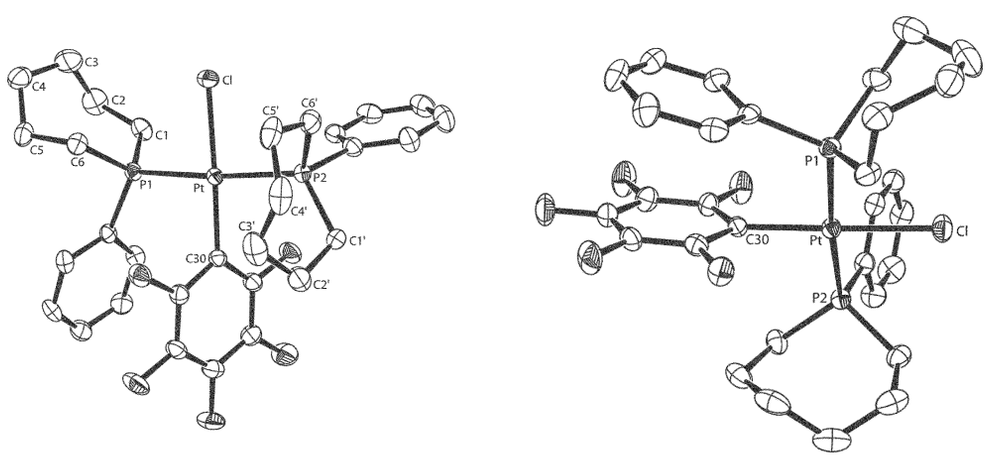

Fig. 5 Molecular structure of **16a**.

Hydrogenation as in Schemes 1 and 6 gave **16a** in 64% yield after workup. The crystal structure was determined as summarized in Table 1 and the experimental section. Metrical parameters are listed in Table 3. The molecular structure is depicted in Fig. 5. There is a single C_6H_5/C_6F_5 π interaction, with a centroid–centroid distance of 3.58 Å.

Complex **11b**, which could cyclize to an eleven-membered interligand metathesis product or a nine-membered intraligand metathesis product, was similarly combined with **2**. However, no tractable products could be isolated, even when reactions were conducted at higher dilution (0.0033 M). Complex **11c** gave similar results in comparable concentration ranges. How-

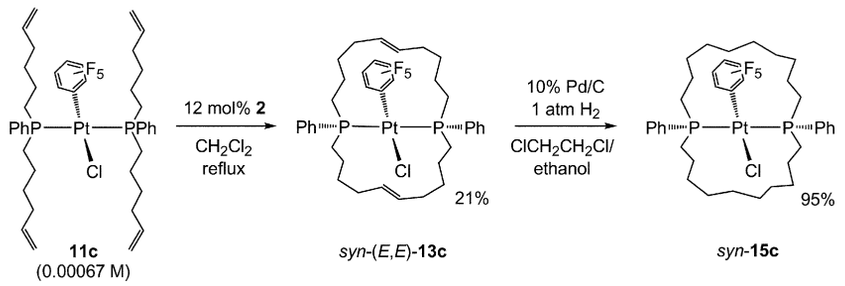

Scheme 9 Ring-closing metathesis/hydrogenation sequence for **11c**.

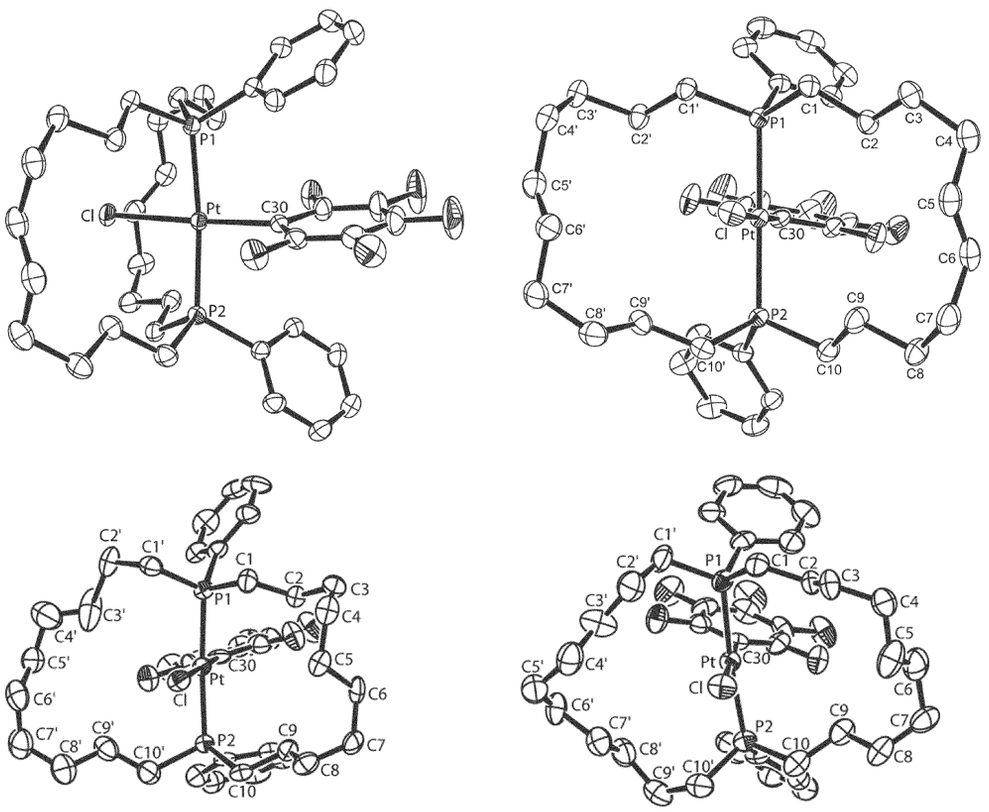

Fig. 6 Molecular structure of *syn*-(*E*,*E*)-**13c** (top left and right) and *syn*-**15c** (bottom left, first independent molecule; bottom right, second independent molecule).

ever, when 0.00067 M solutions were used as shown in Scheme 9, a monoplatinum product could be isolated in 21% yield. A crystal structure established the formation of the intraligand metathesis product *syn*-(*E*,*E*)-**13c**.[19] The molecular structure is depicted in Fig. 6 (top), and metrical parameters are listed in Table 2.

Hydrogenation of *syn*-(*E*,*E*)-**13c** gave the saturated analog *syn*-**15c** in 95% yield. The crystal structure of this compound, a lower homolog of *syn*-**15e** (Fig. 1), was similarly determined. The unit cell contained two independent molecules. As illustrated in Fig. 6 (bottom), they differ in the macrocycle conformations. Both *syn*-(*E*,*E*)-**13c** and *syn*-**15c** exhibit $C_6H_5/C_6F_5/C_6H_5$ π stacking interactions, with average centroid–centroid distances of 4.16 and 3.85–3.94 Å, respectively. They also give a single ^{31}P NMR signal, as expected for *syn* isomers from the analysis in Fig. 4. The ring-closing metathesis of **1c** (Scheme 1), which yields a $P(CH_2)_4CH{=}CH(CH_2)_4P$ bridge as in *syn*-(*E*,*E*)-**13c**, gives a 93 : 7 mixture of *E*/*Z* isomers.

Since **11d** contains a longer methylene segment and interligand metathesis would generate a presumably less strained fifteen-membered ring, enhanced selectivity for cyclization mode **II** was expected. However, only very small amounts of non-oligomeric products could be isolated, even when 0.0019 M solutions of **11d** were treated with **2**. As shown in Scheme 10, the crude reaction mixture was directly hydrogenated. Chromatography gave *syn*-**15d** in 5% overall yield.[19] The *syn* stereochemistry was assigned based upon NMR properties as described above. Although a crystal structure could not be solved, the data were of sufficient quality to exclude the intraligand metathesis product **16d**. Also, no ions derived from loss of a monophosphine ligand were evident in the mass spectrum.

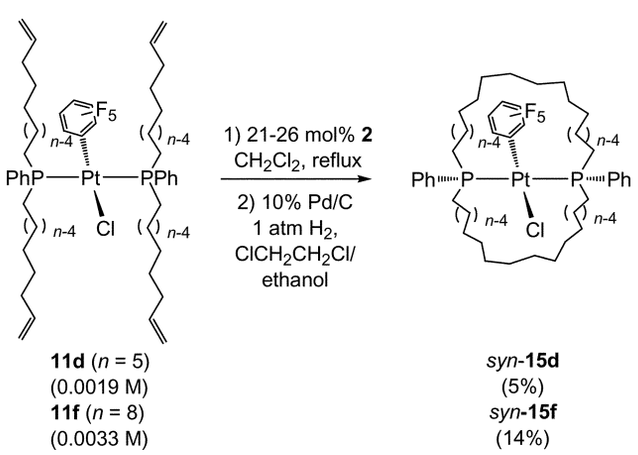

Scheme 10 Ring-closing metathesis/hydrogenation sequences for **11d**,**f**.

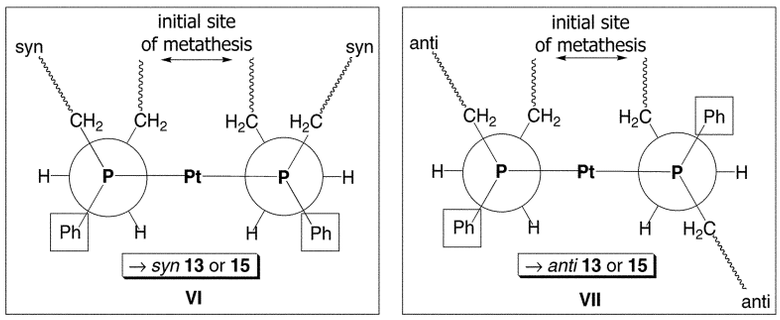

Fig. 7 Some representative conformations of **11** for interligand metathesis.

Given the yield trends in Scheme 1, it was thought that **11f** and **11e** might give comparable amounts of interligand metathesis products. As shown in Scheme 10, the reaction of **11f** (0.0033 M) and **2** was followed by hydrogenation. Chromatography gave *syn*-**15f** in 14% overall yield.[19] Other fractions gave material with ^{31}P NMR signal patterns suggestive of *anti*-**15f**, but samples could not be purified. Since it has not yet been possible to crystallographically characterize *syn*-**15f**, a remote possibility remains that it might be the intraligand metathesis product **16f**. However, the complexes assigned as *syn*-**15c**,**d**,**e**,**f** exhibit several monotonic trends (*e.g.*, ^{31}P NMR 16.2, 12.5, 11.8, 10.8 ppm; J_{PPt} 2612, 2590, 2560, 2551 Hz), in accord with a homologous series.

Discussion

1 Scope and efficiency of macrocyclizations

Schemes 6, 9 and 10 establish that complexes of doubly *trans*-spanning diphosphine ligands are easily accessed by alkene metatheses. Although the yields are modest, advanced generation metathesis catalysts may help in certain cases,[19] and other routes would require many additional steps. Such complexes are to our knowledge unknown. However, as shown in Scheme 11, a conceptually related doubly *trans*-spanning bis(pyridine) complex has also been accessed by alkene metathesis.[20] In the educt **21**, each pyridine nitrogen is flanked by two *ortho* homoallyl groups. These would be expected to extend above and below the palladium square plane, preorganizing the alkenyl moieties for interligand metathesis. Accordingly, **22** is isolated in 80% yield. Hence, alkene metathesis may prove to be a general route to metalladimacrocycles of the type **II** (Scheme 2), albeit in variable yields.

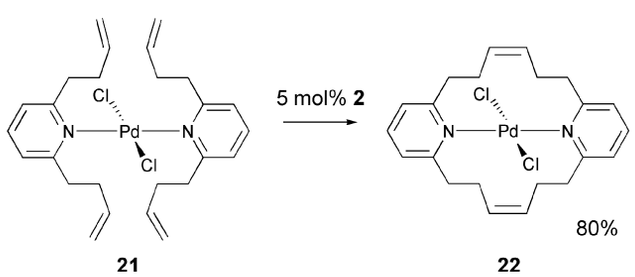

Scheme 11 A doubly *trans*-spanning bis(pyridine) complex.

In earlier papers, we have argued that alkene metatheses in metal coordination spheres are often aided by some analog of the "geminal dialkyl effect".[21] A PPh_2, MPPh, or similar group might play a role analogous to a CR_2 group in making *gauche* conformations of four-atom segments energetically more competitive with *anti* conformations. When only *anti* linkages are present, the termini of α,ω-difunctionalized systems cannot approach one another. Shaw and co-workers have furthermore studied reactions of diphosphines $R_2P(CH_2)_nPR_2$ and square planar complexes that lead to *trans* substitution products.[18] They find that the ratio of monometallic to di- and polymetallic products dramatically increases with the size of the phosphorus substituent.

The PPh_2 and PPhR units in our platinum complexes promote *gauche* conformations in the solid state, as described below. However, for the *mono*macrocyclizations of **1** in Scheme 1, we see no obvious factor that should direct the alkenyl moieties on the same sides of the platinum square plane. Also, no axial bonding interactions involving pendant or bridging C=C (or C≡C)[22] moieties have ever been observed (*e.g.*, *syn*-(*E*,*E*)-**13c**, Fig. 6). Nonetheless, the yields of intramolecular metathesis products are not much lower than with **21**, which as noted above is geometrically predisposed to cyclization. The new data in this paper do not offer additional insight on this point, and pose several further questions, such as: (i) why is intraligand metathesis (**III**, Scheme 2) disfavored in Schemes 6, 9 and 10? (ii) why do the yields of monoplatinum interligand metathesis products drop relative to Scheme 1, despite comparable dilution levels? In analyzing these issues, we presume that our product mixtures are under kinetic control.[19]

Appreciable quantities of intraligand metathesis products are found only with **11a** (Scheme 8), for which interligand metathesis is impossible. Complex **11b**, for which interligand metathesis would also be unlikely, gives exclusively *intermolecular* metathesis. Perhaps intraligand metathesis, which would give a nine-membered cyclic phosphine ligand, is kinetically less favorable than with **11a**, allowing bimolecular condensations to compete. However, with **11c**,**d**,**e**,**f**, all of which give at least some intramolecular metathesis, we have no rationale for the absence of intraligand cyclization. Note that high yields of fifteen-membered cyclic phosphine complexes are obtained by intraligand metathesis in Scheme 3.

Given that intraligand metathesis is not very rapid with **11c**,**d**,**e**,**f**, why are the yields of interligand metathesis products lower than in Scheme 1? Fig. 7 shows two representative conformations of **11** (**VI**, **VII**) as viewed down the phosphorus–carbon bond axes, the energies of which should be nearly equal. The chlorine and C_6F_5 ligands can be visualized as directly behind and in front of the "Pt". In both cases, *gauche* Pt–PPhR–CH_2–CH_2 conformations are used to direct two $(CH_2)_nCH{=}CH_2$ moieties on the same side of the platinum square plane, and in orientations that are favorable for interligand metathesis. Many other conformations are possible that are to varying degrees less favorable for macrocyclization, as analyzed elsewhere.[23]

Importantly, **VI** can only lead to *syn* isomers of **13**, whereas **VII** can only lead to *anti* isomers. Hence, the *syn*/*anti* stereochemistry is set by the first metathesis. Furthermore, in the macrocycle resulting from **VII**, the two remaining $(CH_2)_n$-$CH{=}CH_2$ moieties will be directed on opposite sides of the platinum square plane, an orientation unfavorable for intramolecular metathesis. Thus, bimolecular condensations should be more competitive, and more oligomeric products should arise from this manifold. This would result in lower yields of monoplatinum interligand metathesis products. Accordingly, only in the case of **15e** is an *anti* isomer isolated. Finally, we note in passing that it might be easier to incorporate a C_6H_5/

C_6F_5/C_6H_5 π stacking interaction into the transition state derived from **VI**.

2 Macrocycle structures

Various crystallographic features are relevant to phenomena analyzed above. First, the interligand metathesis products in Table 2 have bond lengths and angles about platinum similar to those of the intraligand metathesis products in Table 3. The P–Pt–P bond angles (177.99(4)–172.21(10)° *vs*. 175.54(3)–174.84(3)°) might have contracted if the ring strain associated with the *trans*-spanning ligands were significant.

Consider the torsion angle patterns of the complexes in Table 2 next. With *syn*-**15e**, the macrocycles are homologous. All four Pt–PPh–CH_2–CH_2 segments (Pt–P(1)–C(1)–C(2), C(13)–C(14)–P(2)–Pt, and primed analogs) exhibit *gauche* conformations with torsion angles of 46.5/56.5° and 56.0/39.2°. This is in accord with an analog of a "germinal dialkyl effect" as discussed in the previous section, and as exploited in the cyclization-favorable conformations in Fig. 7. All of the macrocycles in Scheme 1 (**3c**,**e**,**f**,**g**) crystallize similarly. The four PPh–CH_2–CH_2–CH_2 segments in *syn*-**15e** exhibit *anti* conformations, with torsion angles of −175.3/−164.6° and −169.7/−172.2°. The three subsequent four-carbon sequences in each ring also show *anti* conformations. However, of the five remaining four-carbon sequences, four exhibit *gauche* conformations, with torsion angles of −51.7/−60.6°, −62.1/−67.0°, −61.9/−60.5°, and −59.7/−50.4°.

The torsion angle patterns of the macrocycles in *anti*-**15e** are not homologous, and differ significantly from those of *syn*-**15e**. One of the two Pt–PPh–CH_2–CH_2 segments in each ring now exhibits a *gauche* conformation (C(13)–C(14)–P(2)–Pt −53.6°; Pt–P(1)–C(1′)–C(2′) −44.7°), while the other remains *anti* (−160.1°, 167.6°). All PPh–CH_2–CH_2–CH_2 sequences again show *anti* conformations. However, now there are six four-carbon *gauche* segments in each ring, for a total of seven *gauche* moieties – one more than in each ring of *syn*-**15e**. Although an ensemble of accessible conformations would be expected in solution, this suggests (in the absence of non-bonded interactions) that *anti*-**15e** is more highly strained. As summarized in Table 3, each fifteen-membered ring in the constitutional isomer **16e** exhibits seven four-carbon *gauche* segments. Furthermore, all C(13)–C(14)–P–C(1) and C(14)–P–C(1)–C(2) sequences have *gauche* conformations (50.3/−46.1°, 57.0/−63.1°), consistent with a PPhPt-based "geminal dialkyl effect".

Complex *syn*-**15c**, with two thirteen-membered rings, crystallizes with two independent molecules in the unit cell. Although none of the torsion angle patterns are homologous, all eight Pt–PPh–CH_2–CH_2 segments exhibit *gauche* conformations, with torsion angles of ±36.9° to ±82.7°. Two of the four rings exhibit three additional *gauche* PPh–CH_2–CH_2–CH_2 or four-carbon segments, and the other rings exhibit four and five. The unsaturated analog *syn*-(*E,E*)-**13c** also crystallizes with *gauche* Pt–PPh–CH_2–CH_2 segments. One ring features only two additional *gauche* segments, and the other three (four-carbon in each case). The *Z* C=C moiety enforces one *anti* linkage.

A final structural issue involves the size relationship between the macrocycle and the other ligands on platinum. Consider first **3e** (Scheme 1), which has a single *trans*-spanning $P(CH_2)_{14}P$ bridge. A 180° rotation of the Cl–Pt–C_6F_5 moiety, with the smaller chlorine ligand passing under the bridge, is rapid on the NMR time scale and renders diastereotopic groups equivalent.[3d] In **3c**, which has a shorter $P(CH_2)_{10}P$ bridge, the rotational barrier becomes much higher and separate NMR signals for diastereotopic groups are observed. As can be visualized from **V** in Fig. 4, analogous 180° rotations would also exchange the diastereotopic phosphorus atoms of *anti*-**15e**. However, since there are now two $P(CH_2)_{14}P$ bridges, the larger C_6F_5 group must also be able to pass under the methylene chain.

The distance from the platinum to the *para* fluorine atom in *anti*-**15e** is 6.18 Å. This is nearly as great as the distance from platinum to the most remote macrocyclic carbons (7.19/6.85 Å). When the van der Waals radius of fluorine (1.47 Å) is added to the former value, and the van der Waals radius of carbon (1.70 Å) is subtracted from the latter values,[24] it is obvious that the "vehicle height" is much greater than the "bridge height" (7.65 Å *vs*. 5.49/5.15 Å). Accordingly, two ^{31}P NMR signals are observed. However, with still longer methylene bridges, rotation of the Cl–Pt–C_6F_5 moiety should become possible, leading to dynamic NMR phenomena.

3 Summary and prospective

Architecturally novel doubly *trans*-spanning diphosphine complexes are easily accessed by interligand alkene metatheses of the bis(phosphine) complexes **11c**,**d**,**e**,**f** (Schemes 6, 9 and 10). Although the yields are lower than those of the singly *trans*-spanning diphosphine complexes obtained from **1c**,**e**,**f**,**g** (Scheme 1), advanced-generation metatheses catalysts may offer improvements.[19] In any event, conventional syntheses would require many additional steps. Curiously, intraligand metathesis products are observed only when the carbon bridges would be too short to span *trans* positions (Scheme 8). One attempt to extend these reactions to still more complex educts that can lead to higher polycycles was disappointing (Scheme 4). However, as will be described in future papers, others have been spectacularly successful.[25] Taken together, these investigations – as well as clever findings by others[2,5] – are significantly advancing the utility of alkene metatheses in syntheses of topologically unusual inorganic and organometallic systems.

Experimental

General data

All reactions were conducted under N_2 (or H_2) atmospheres. Chemicals were treated as follows: THF, ether, benzene, and toluene, distilled from Na/benzophenone; CH_2Cl_2, distilled from CaH_2 (for reactions) or simple distillation (chromatography); hexanes and ethanol, simple distillation; $HNEt_2$, distilled from NaOH; $CDCl_3$, $ClCH_2CH_2Cl$ (99%, Fluka), $Ru(=CHPh)(PCy_3)_2(Cl)_2$ (**2**, Strem), $H_3B{\cdot}SMe_2$ (Fluka, 99%), $Rh(PPh_3)_3(Cl)$ (Strem), 10% Pd/C (Lancaster or Acros), $PPhH_2$ (99%, Strem), *n*-BuLi (Acros, 2.5 M in hexanes), $Br(CH_2)_nCH=CH_2$ (*n* = 2, 98%, Fluka; 3, 95%, Aldrich; 4, 90%, Fluka; 5, 97%, Aldrich), used as received.

NMR spectra were obtained on Bruker or Jeol 400 MHz spectrometers. IR and mass spectra were recorded on ASI React-IR 1000 and Micromass Zabspec instruments, respectively. DSC and TGA data were obtained with a Mettler-Toledo DSC-821 instrument.[26] Microanalyses were conducted with a Carlo Erba EA1110 instrument (in-house).

$PPh((CH_2)_2CH=CH_2)_2$ (4a)[7]

A Schlenk flask was charged with $PPhH_2$ (0.514 g, 4.67 mmol) and THF (20 mL) and cooled to 0 °C. Then *n*-BuLi (2.5 M in hexanes, 3.75 mL, 9.4 mmol) was added dropwise with stirring over 10 min. The colorless solution turned yellow–orange. After 5 min, $Br(CH_2)_2CH=CH_2$ (0.95 mL, 9.4 mmol) was added. The solution became colorless. The cold bath was removed. After 3.5 h, solvent was removed by oil-pump vacuum. The residue was filtered through a silica plug (5 cm) with hexanes–toluene (1 : 1 v/v). The filtrate was taken to dryness by oil-pump vacuum to give **4a** (0.916 g, 4.20 mmol, 90%) as a colorless oil. Calc. for $C_{14}H_{19}P$: C, 77.06; H, 8.72. Found: C, 77.54; H, 9.51%.

NMR:[27] ^{1}H 7.56–7.52 (m, 2 H of Ph), 7.37 (m, 3 H of Ph), 5.92–5.82 (m, 2 H, 2CH=), 5.05–4.96 (m, 4 H, 2 =CH_2), 2.17–2.10 (m, 4 H, 2CH_2), 1.85–1.79 (m, 4 H, 2CH_2); ^{13}C{^{1}H}[28] 139.3 (d, J_{CP} = 11.9, CH=), 138.4 (d, $^1J_{CP}$ = 14.7, *i*-Ph), 132.9 (d, $^2J_{CP}$ = 18.8, *o*-Ph), 129.3 (s, *p*-Ph), 128.8 (d, $^3J_{CP}$ = 7.0, *m*-Ph), 114.8 (s, =CH_2), 30.4 (d, J_{CP} = 14.8, CH_2), 27.8 (d, J_{CP} = 11.9, CH_2); ^{31}P{^{1}H} −23.0 (s).

PPh((CH$_2$)$_3$CH=CH$_2$)$_2$ (4b)[8]

$PPhH_2$ (0.685 g, 6.23 mmol), THF (20 mL), *n*-BuLi (2.5 M in hexanes, 5.0 mL, 12.5 mmol) and Br(CH_2)$_3$CH=CH_2 (1.48 mL, 12.5 mmol) were combined in a procedure analogous to that for **4a**. An identical workup gave **4b** (1.41 g, 5.73 mmol, 92%) as a colorless oil.

NMR:[27] ^{1}H 7.55–7.51 (m, 2 H of Ph), 7.38–7.35 (m, 3 H of Ph), 5.81–5.73 (m, 2 H, 2CH=), 5.04–4.96 (m, 4 H, 2 =CH_2), 2.17–2.12 (m, 4 H, 2CH_2), 1.76–1.70 (m, 4 H, 2CH_2), 1.54–1.48 (m, 4 H, 2CH_2); ^{13}C{^{1}H}[28] 138.8 (d, $^1J_{CP}$ = 15.0, *i*-Ph), 138.4 (s, CH=), 132.6 (d, $^2J_{CP}$ = 18.3, *o*-Ph), 128.9 (s, *p*-Ph), 128.5 (d, $^3J_{CP}$ = 7.0, *m*-Ph), 115.0 (s, =CH_2), 35.4 (d, J_{CP} = 11.8, CH_2), 27.8 (d, J_{CP} = 10.8, CH_2), 25.4 (d, J_{CP} = 14.3, CH_2); ^{31}P{^{1}H} −23.5 (s).

PPh((CH$_2$)$_4$CH=CH$_2$)$_2$ (4c)

$PPhH_2$ (0.572 g, 5.20 mmol), THF (20 mL), *n*-BuLi (2.5 M in hexanes, 4.2 mL, 10.5 mmol) and Br(CH_2)$_4$CH=CH_2 (1.4 mL, 10.4 mmol) were combined in a procedure analogous to that for **4a**. An identical workup gave **4c** (1.27 g, 4.63 mmol, 89%) as a colorless oil. Calc. for $C_{18}H_{27}P$: C, 78.83; H, 9.85. Found C, 79.11; H, 10.04%.

NMR:[27] ^{1}H 7.44 (m, 2 H of Ph), 7.26 (m, 3 H of Ph), 5.67 (m, 2 H, 2CH=), 4.86 (m, 4 H, 2 =CH_2), 1.98–1.91 (m, 4 H, 2CH_2), 1.64–1.59 (m, 4 H, 2CH_2), 1.42–1.29 (m, 8 H, 4CH_2); ^{13}C{^{1}H}[28] 139.1 (s, CH=), 138.6 (d, $^1J_{CP}$ = 16.0, *i*-Ph), 132.7 (d, $^2J_{CP}$ = 19.0, *o*-Ph), 129.1 (s, *p*-Ph), 128.7 (d, $^3J_{CP}$ = 7.0, *m*-Ph), 114.8 (s, =CH_2), 33.8 (s, CH_2), 30.8 (d, J_{CP} = 11.0, CH_2), 28.4 (d, J_{CP} = 11.0, CH_2), 25.8 (d, J_{CP} = 13.0, CH_2); ^{31}P{^{1}H} −23.0 (s).

MS:[29] 275 (**4c**$^+$, 100%), 192 ([**4c** − (CH$_2$)$_4$CH=CH$_2$]$^+$, 92%).

PPh((CH$_2$)$_5$CH=CH$_2$)$_2$ (4d)

$PPhH_2$ (0.606 g, 5.51 mmol), THF (20 mL), *n*-BuLi (2.5 M in hexanes, 4.5 mL, 11.3 mmol) and Br(CH_2)$_5$CH=CH_2 (1.73 mL, 11.4 mmol) were combined in a procedure analogous to that for **4a**. An identical workup gave **4d** (1.55 g, 5.12 mmol, 93%) as a colorless oil. Calc. for $C_{20}H_{31}P$: C, 79.47; H, 10.26. Found C, 78.89; H, 10.61%.

NMR:[27] ^{1}H 7.54–7.53 (m, 2 H of Ph), 7.38–7.36 (m, 3 H of Ph), 5.82–5.80 (m, 2 H, 2CH=), 5.02–4.94 (m, 4 H, 2 =CH_2), 2.05–2.00 (m, 4 H, 2CH_2), 1.73–1.70 (m, 4 H, 2CH_2), 1.45–1.36 (m, 12 H, 6CH_2); ^{13}C{^{1}H}[28] 139.4 (d, $^1J_{CP}$ = 18.3, *i*-Ph), 139.3 (s, CH=), 132.7 (d, $^2J_{CP}$ = 18.4, *o*-Ph), 129.0 (s, *p*-Ph), 128.6 (d, $^3J_{CP}$ = 6.7, *m*-Ph), 114.7 (s, =CH_2), 34.0 (s, CH_2), 31.1 (d, J_{CP} = 11.5, CH_2), 29.0 (s, CH_2), 28.6 (d, J_{CP} = 11.0, CH_2), 26.2 (d, J_{CP} = 13.6, CH_2); ^{31}P{^{1}H} −23.3 (s).

MS:[29] 303 (**4d**$^+$, 100%), 206 ([**4d** − (CH$_2$)$_5$CH=CH$_2$]$^+$, 62%).

PPh((CH$_2$)$_8$CH=CH$_2$)$_2$ (4f)

$PPhH_2$ (0.152 g, 1.38 mmol), THF (10 mL), *n*-BuLi (2.5 M in hexanes, 1.1 mL, 2.8 mmol) and Br(CH_2)$_8$CH=CH_2 (0.55 mL, 2.75 mmol)[3d] were combined in a procedure analogous to that for **4a**. An identical workup gave **4f** (0.521 g, 1.35 mmol, 98%) as a colorless oil.[30]

NMR:[27] ^{1}H 7.52 (m, 2 H of Ph), 7.36 (m, 3 H of Ph), 5.80 (m, 2 H, 2CH=), 5.03–4.92 (m, 4 H, 2 =CH_2), 2.08–2.00 (m, 4 H, 2CH_2), 1.37–1.27 (m, 28 H, 14CH_2); ^{13}C{^{1}H}[28] 139.6 (s, CH=), 139.5 (d, $^1J_{CP}$ = 19.9, *i*-Ph), 132.7 (d, $^2J_{CP}$ = 18.3, *o*-Ph), 128.9 (s, *p*-Ph), 128.6 (d, $^3J_{CP}$ = 9.1, *m*-Ph), 114.5 (s, =CH_2), 34.2 (s, CH_2), 31.6 (d, J_{CP} = 11.5, CH_2), 29.7 (s, CH_2), 29.6 (s, CH_2), 29.5 (s, CH_2), 29.3 (s, CH_2), 28.7 (d, J_{CP} = 10.9, CH_2), 26.3 (d, J_{CP} = 13.4, CH_2); ^{31}P{^{1}H} −23.2 (s).

MS:[29] 387 (**4f**$^+$, 100%).

***trans*-(Cl)(C$_6$F$_5$)Pt(PPh((CH$_2$)$_2$CH=CH$_2$)$_2$)$_2$ (11a)**

A Schlenk flask was charged with [Pt(μ-Cl)(C$_6$F$_5$)(S(CH_2-CH_2)$_2$)]$_2$ (**12**; 0.460 g, 0.474 mmol),[9] **4a** (0.424 g, 1.945 mmol) and CH_2Cl_2 (30 mL). The pale green mixture was stirred (14 h) and became colorless. Solvent was removed by oil-pump vacuum. The residue was filtered through neutral alumina (3.0 × 2.5 cm column) using 1 : 1 v/v CH_2Cl_2–hexanes. Solvent was removed from the product fraction by oil-pump vacuum to yield **11a** as a colorless oil (0.627 g, 0.752 mmol, 79%). Calc. for $C_{34}H_{38}ClF_5P_2Pt$: C, 48.95; H, 4.56. Found: C, 49.33; H, 4.80%.

NMR:[27] ^{1}H 7.44 (m, 4 H of 2Ph), 7.35 (m, 6 H of 2Ph), 5.84–5.75 (m, 4 H, 4CH=), 5.03–4.97 (m, 8 H, 4 =CH_2), 2.37–2.27 (m, 8 H, 4CH_2), 2.19–2.09 (m, 8 H, 4CH_2); ^{13}C{^{1}H}[31a,32,33] 137.8 (virtual t,[34] J_{CP} = 7.5, CH=), 131.6 (virtual t,[34] J_{CP} = 5.3, *o*-Ph), 130.6 (s, *p*-Ph), 130.0 (virtual t,[34] J_{CP} = 26.0, *i*-Ph), 128.7 (virtual t,[34] J_{CP} = 4.8, *m*-Ph), 115.6 (s, =CH_2), 28.4 (s, PCH$_2$*C*H$_2$), 22.6 (virtual t,[34] J_{CP} = 16.4, PCH_2); ^{31}P{^{1}H} 10.7 (s, J_{PPt} = 2564).[35]

IR (cm^{-1}, oil film) 3080 (w), 2980 (w), 2934 (w), 2864 (w), 1640 (m), 1502 (s), 1459 (s), 1436 (s), 1108 (m), 1058 (m), 953 (s), 911 (s), 803 (s), 722 (s), 687 (s). MS:[29] 798 ([**11a** − Cl]$^+$, 100%), 579 ([**11a** − Cl − **4a**]$^+$, 40%), 411 ([**11a** − Cl − C$_6$F$_5$ − **4a**]$^+$, 80%), 219 (**4a**$^+$, 80%), 164 ([**4a** − (CH$_2$)$_4$CH=CH$_2$]$^+$, 70%).

***trans*-(Cl)(C$_6$F$_5$)Pt(PPh((CH$_2$)$_3$CH=CH$_2$)$_2$)$_2$ (11b)**

Complex **12** (0.430 g, 0.443 mmol), **4b** (0.440 g, 1.79 mmol) and CH_2Cl_2 (25 mL) were combined in a procedure analogous to that for **11a** (17 h stirring). An identical workup gave **11b** as a colorless oil (0.675 g, 0.759 mmol, 86%). Calc. for $C_{38}H_{46}ClF_5P_2Pt$: C, 51.27; H, 5.17. Found: C, 50.48; H, 5.12%.

NMR:[27] ^{1}H 7.47–7.43 (m, 4 H of 2Ph), 7.35–7.30 (m, 6 H of 2Ph), 5.76–5.66 (m, 4 H, 4CH=), 5.02–4.98 (m, 8 H, 4 =CH_2), 2.19–2.07 (m, 12 H, 6CH_2), 2.00–1.96 (m, 4 H, 2CH_2), 1.81–1.70 (m, 4 H, 2CH_2), 1.50–1.42 (m, 4 H, 2CH_2); ^{13}C{^{1}H}[31,32,33] 137.6 (s, CH=), 131.5 (virtual t,[34] J_{CP} = 5.3, *o*-Ph), 130.2 (s, *p*-Ph), 128.4 (virtual t,[34] J_{CP} = 4.8, *m*-Ph), 115.8 (s, =CH_2), 35.1 (virtual t,[34] J_{CP} = 7.1, PCH$_2$CH$_2$*C*H$_2$), 23.3 (s, PCH$_2$*C*H$_2$), 22.5 (virtual t,[34] J_{CP} = 16.8, PCH_2); ^{31}P{^{1}H} 10.2 (s, J_{PPt} = 2551).[35]

IR (cm^{-1}, oil film) 3080 (w), 2980 (w), 2934 (w), 2864 (w), 1640 (m), 1502 (s), 1459 (s), 1436 (s), 1108 (m), 1058 (m), 953 (s), 911 (s), 803 (s), 722 (s), 687 (s). MS:[29] 854 ([**11b** − Cl]$^+$, 80%), 606 ([**11b** − Cl − **4b**]$^+$, 40%), 440 ([**11b** − Cl − C$_6$F$_5$ − **4b**]$^+$, 100%), 245 (**4b**$^+$, 80%), 178 ([**4b** − (CH$_2$)$_3$CH=CH$_2$]$^+$, 100%).

***trans*-(Cl)(C$_6$F$_5$)Pt(PPh((CH$_2$)$_4$CH=CH$_2$)$_2$)$_2$ (11c)**

Complex **12** (0.522 g, 0.537 mmol), **4c** (0.495 g, 1.81 mmol) and CH_2Cl_2 (30 mL) were combined in a procedure analogous to that for **11a** (18 h stirring). An identical workup gave **11c** as a colorless oil (0.738 g, 0.780 mmol, 73%). Calc. for $C_{42}H_{54}ClF_5P_2Pt$: C, 53.31; H, 5.71. Found: C, 53.45; H, 5.85%.

NMR:[27] ^{1}H 7.39 (m, 4 H of 2Ph), 7.29 (m, 6 H of 2Ph), 5.71–5.60 (m, 4 H, 4CH=), 4.94–4.84 (m, 8 H, 4 =CH_2), 2.20–2.10 (m, 4 H, 2CH_2), 2.03–1.96 (m, 12 H, 6CH_2), 1.62–1.51 (m, 4 H, 2CH_2), 1.44–1.32 (m, 12 H, 6CH_2); ^{13}C{^{1}H}[31a,32,33] 138.6 (s, CH=), 131.6 (virtual t,[34] J_{CP} = 5.1, *o*-Ph), 130.6 (virtual t,[34] J_{CP} = 25.9, *i*-Ph), 130.3 (s, *p*-Ph), 128.5 (virtual t,[34] J_{CP} = 4.7, *m*-Ph), 115.2 (s, =CH_2), 33.6 (s, CH_2), 30.7 (virtual t,[34] J_{CP} = 6.9, PCH$_2$CH$_2$*C*H$_2$), 23.6 (s, CH_2), 22.9 (virtual t,[34] J_{CP} = 16.6, PCH_2); ^{31}P{^{1}H} 10.1 (s, J_{PPt} = 2543).[35]

IR (cm^{-1}, oil film) 3080 (w), 2930 (m), 2860 (w), 1640 (w), 1502 (s), 1459 (s), 1440 (s), 1108 (m), 1061 (s), 957 (s), 911 (s), 799 (s), 741 (s), 695 (s). MS:[29] 910 ([**11c** − Cl]$^+$, 40%), 741 ([**11c** − Cl − C$_6$F$_5$]$^+$, 20%), 467 ([**11c** − Cl − C$_6$F$_5$ − **4c**]$^+$, 50%), 385

([**11c** − Cl − C_6F_5 − **4c** − $(CH_2)_4CH{=}CH_2$]$^+$, 45%), 275 (**4c**$^+$, 70%), 192 ([**4c** − $(CH_2)_4CH{=}CH_2$]$^+$, 100%).

trans-(Cl)(C_6F_5)Pt(PPh((CH_2)$_5$CH=CH_2)$_2$)$_2$ (11d)

Complex **12** (0.260 g, 0.268 mmol), **4d** (0.340 g, 1.13 mmol) and CH_2Cl_2 (20 mL) were combined in a procedure analogous to that for **11a**. An identical workup gave **11d** as a colorless oil (0.497 g, 0.496 mmol, 93%). Calc. for $C_{46}H_{62}ClF_5P_2Pt$: C, 55.12; H, 6.19. Found: C, 54.75; H, 6.50.

NMR:[27] ^{1}H 7.43–7.41 (m, 4 H of 2Ph), 7.34–7.28 (m, 6 H of 2Ph), 5.82–5.75 (m, 4 H, 4CH=), 5.01–4.93 (m, 8 H, 4 =CH_2), 2.20–2.12 (m, 4 H, 2CH_2), 2.01–1.95 (m, 12 H, 6CH_2), 1.70–1.55 (m, 4 H, 2CH_2), 1.45–1.30 (m, 20 H, 10CH_2); ^{13}C{^{1}H} [31a,32,33] 139.1 (s, CH=), 131.6 (virtual t,[34] J_{CP} = 5.1, *o*-Ph), 130.7 (virtual t,[34] J_{CP} = 26.1, *i*-Ph), 130.3 (s, *p*-Ph), 128.5 (virtual t,[34] J_{CP} = 4.6, *m*-Ph), 114.9 (s, =CH_2), 33.9 (s, CH_2), 31.0 (virtual t,[34] J_{CP} = 7.0, $PCH_2CH_2CH_2$), 28.7 (s, CH_2), 24.1 (s, CH_2), 23.1 (virtual t,[34] J_{CP} = 16.7, PCH_2); ^{31}P{^{1}H} 10.2 (s, J_{PPt} = 2543).[35]

IR (cm^{-1}, oil film) 3080 (w), 2930 (m), 2856 (m), 1640 (m), 1502 (s), 1459 (s), 1440 (s), 1061 (s), 957 (s), 907 (s), 799 (s), 741 (s), 694 (s). MS:[29] 966 ([**11d** − Cl]$^+$, 20%), 797 ([**11d** − Cl − C_6F_5]$^+$, 20%), 495 ([**11d** − Cl − C_6F_5 − **4d**]$^+$, 60%), 397 ([**11d** − Cl − C_6F_5 − **4d** − $(CH_2)_5CH{=}CH_2$]$^+$, 50%), 303 (**4d**$^+$, 100%), 192 ([**4d** − $(CH_2)_5CH{=}CH_2$]$^+$, 70%).

trans-(Cl)(C_6F_5)Pt(PPh((CH_2)$_6$CH=CH_2)$_2$)$_2$ (11e)

Complex **12** (0.416 g, 0.430 mmol), **4e** (0.568 g, 1.719 mmol)[3c] and CH_2Cl_2 (30 mL) were combined in a procedure analogous to that for **11a** (16 h stirring). A similar workup (2.5 × 2.5 cm column, 3 : 1 v/v CH_2Cl_2–hexanes) gave **11e** as a colorless oil (0.824 g, 0.779 mmol, 91%). Calc. for $C_{50}H_{70}ClF_5P_2Pt$: C, 56.73; H, 6.66. Found: C, 56.12; H, 6.58%.

NMR:[27] ^{1}H 7.40–7.37 (m, 4 H of 2Ph), 7.30–7.26 (m, 6 H of 2Ph), 5.81–5.68 (m, 4 H, 4CH=), 4.98–4.89 (m, 8 H, 4=CH_2), 2.10–2.09 (m, 4 H, 4PC*H*H′), 2.01–1.89 (m, 12 H, 4PCH*H*′, 4CH_2CH=), 1.60–1.56 (m, 4 H, 4PCH_2C*H*H′), 1.34–1.24 (m, 28 H, 4PCH_2CH*H*′, 12CH_2); ^{13}C{^{1}H} [31a,32,33] 138.9 (s, CH=), 131.2 (virtual t,[34] J_{CP} = 5.1, *o*-Ph), 130.4 (virtual t,[34] J_{CP} = 25.8, *i*-Ph), 129.9 (s, *p*-Ph), 128.0 (virtual t,[34] J_{CP} = 4.4, *m*-Ph), 114.3 (=CH_2), 33.7 (s, *C*H_2CH=), 31.0 (virtual t,[34] J_{CP} = 6.5, $PCH_2CH_2CH_2$), 28.7 (s, CH_2), 28.6 (s, CH_2), 23.7 (s, CH_2), 22.7 (virtual t,[34] J_{CP} = 16.5, PCH_2); ^{31}P{^{1}H} 9.3 (s, $^1J_{PPt}$ = 2540).[35]

IR (cm^{-1}, powder film) 3080 (w), 2930 (m), 2856 (w), 1502 (s), 1463 (s), 1436 (s), 1104 (m), 1061 (m), 1000 (m), 953 (s), 911 (s), 803 (m), 741 (s), 690 (s). MS:[29] 1059 (**11e**$^+$, 2%), 1022 ([**11e** − Cl]$^+$, 40%), 853 ([**11e** − Cl − C_6F_5]$^+$, 22%), 489 ([**11e** − Cl − C_6F_5 − **4e**]$^+$, 70%), 331 (**4e**$^+$, 100%).

trans-(Cl)(C_6F_5)Pt(PPh((CH_2)$_8$CH=CH_2)$_2$)$_2$ (11f)

Complex **12** (0.504 g, 0.519 mmol), **4f** (0.839 g, 2.17 mmol) and CH_2Cl_2 (30 mL) were combined in a procedure analogous to that for **11a** (15 h stirring). An identical workup gave **11f** as a colorless oil (0.898 g, 0.768 mmol, 74%). Calc. for $C_{58}H_{86}ClF_5P_2Pt$: C, 59.80; H, 7.72. Found: C, 59.52; H, 7.35%.

NMR:[27] ^{1}H 7.43 (m, 4 H of 2Ph), 7.29 (m, 6 H of 2Ph), 5.82 (m, 4 H, 4CH=), 4.98 (m, 8 H, 4 =CH_2), 2.14–1.94 (m, 16 H, 8CH_2), 1.58 (m, 4 H, 2CH_2), 1.37–1.25 (m, 44 H, 22CH_2); ^{13}C{^{1}H} [31a,32,33] 139.4 (s, CH=), 131.4 (virtual t,[34] J_{CP} = 5.1, *o*-Ph), 130.7 (virtual t,[34] J_{CP} = 25.6, *i*-Ph), 130.0 (s, *p*-Ph), 128.2 (virtual t,[34] J_{CP} = 4.7, *m*-Ph), 114.3 (s, =CH_2), 34.0 (s, CH_2), 31.4 (virtual t,[34] J_{CP} = 6.9, $PCH_2CH_2CH_2$), 29.7 (s, CH_2), 29.3 (s, CH_2), 29.3 (s, CH_2), 29.0 (s, CH_2), 24.0 (s, CH_2), 22.9 (virtual t,[34] J_{CP} = 16.5, PCH_2); ^{31}P{^{1}H} 10.1 (s, J_{PPt} = 2540).[35]

IR (cm^{-1}, oil film) 3080 (w), 2926 (s), 2856 (s), 1640 (w), 1502 (s), 1459 (s), 1061 (m), 957 (s), 907 (s), 799 (m), 741 (s), 695 (s). MS:[29] 1134 ([**11f** − Cl]$^+$, 100%), 965 ([**11f** − Cl − C_6F_5]$^+$, 70%).

Metathesis of 11a; (*Z*,*Z*)-*trans*-(Cl)(C_6F_5)Pt-(PPh(CH_2)$_2$CH=CH(CH_2)$_2$)$_2$ ((*Z*,*Z*)-14a)

A two-necked flask was charged with **11a** (0.465 g, 0.558 mmol), Grubbs' catalyst **2** (*ca*. half of 0.036 g, 0.0390 mmol, 14 mol%) and CH_2Cl_2 (60 mL; the resulting solution is 0.0093 M in **11a**), and fitted with a condenser. The solution was refluxed. After 2 h, the remaining **2** was added. After 2 h, solvent was removed by oil-pump vacuum. The residue was filtered through neutral alumina (2.5 × 2.5 cm column) using CH_2Cl_2. Solvent was removed from the filtrate by oil-pump vacuum to give (*Z*,*Z*)-**14a** as a pale pink solid (0.371 g, 0.477 mmol, 86%), mp 218–220 °C (decomp.) (capillary). Calc. for $C_{30}H_{30}ClF_5P_2Pt$: C, 46.31; H, 3.86. Found: C, 46.81; H, 4.28%.

NMR:[27] ^{1}H 7.45–7.39 (m, 4 H of 2Ph), 7.35–7.28 (m, 6 H of 2Ph), 5.79–5.75 (m, 4 H, 2CH=CH), 2.55–2.43 (m, 8 H, 4CH_2), 2.32–2.20 (m, 8 H, 4CH_2); ^{13}C{^{1}H} [31a,32] 131.8 (s, CH=CH), 131.3 (virtual t,[34] J_{CP} = 4.8, *o*-Ph), 130.4 (virtual t,[34] J_{CP} = 25.9, *i*-Ph), 130.3 (s, *p*-Ph), 128.8 (virtual t,[34] J_{CP} = 4.8, *m*-Ph), 22.4 (s, CH_2), 21.5 (virtual t,[34] J_{CP} = 16.1, CH_2); ^{31}P{^{1}H} 15.8 (s, J_{PPt} = 2511).[35]

IR (cm^{-1}, powder film) 3030 (w), 2930 (w), 2856 (w), 1502 (s), 1459 (s), 1058 (m), 953 (s), 718 (s), 695 (s). MS:[29] 742 ([**14a** − Cl]$^+$, 100%), 552 ([**14a** − Cl − PhP((CH_2)CH=CH(CH_2))]$^+$, 30%).

trans-(Cl)(C_6F_5)Pt(PPh((CH_2)$_6$)$_2$ (16a)

A two-necked flask was charged with **14a** (0.371 g, 0.477 mmol), 10% Pd/C (0.064 g, 0.0601 mmol Pd), $ClCH_2CH_2Cl$ (20 mL) and ethanol (20 mL), flushed with H_2, and fitted with a balloon of H_2. The mixture was stirred for 69 h. Solvent was removed by oil-pump vacuum. The residue was filtered through neutral alumina (2.5 × 2.5 cm column) using 3 : 1 v/v hexanes–CH_2Cl_2. Solvent was removed from the filtrate by oil-pump vacuum to give **16a** as a white powder (0.240 g, 0.307 mmol, 64%), mp 145 °C (capillary), 147 °C (DSC; T_i/T_e/T_p/T_e/T_f 120.7/145.3/147.0/149.0/179.8 °C). TGA: onset of mass loss, 285 °C (T_e). Calc. for $C_{30}H_{34}ClF_5P_2Pt$: C, 46.07; H, 4.35. Found: C, 45.98; H, 4.43%.

NMR:[27] ^{1}H 7.44 (m, 4 H of 2Ph), 7.28 (m, 6 H of 2Ph), 2.52–2.58 (m, 4 H, 2CH_2), 2.28–2.24 (m, 4 H, 2CH_2), 1.91–1.88 (m, 4 H, 2CH_2), 1.70–1.65 (m, 8 H, 4CH_2), 1.55–1.53 (m, 4 H, 2CH_2); ^{13}C{^{1}H} [31a,32] 132.1 (virtual t,[34] J_{CP} = 25.4, *i*-Ph), 131.2 (virtual t,[34] J_{CP} = 4.8, *o*-Ph), 130.0 (s, *p*-Ph), 128.5 (virtual t,[34] J_{CP} = 4.7, *m*-Ph), 29.3 (s, CH_2), 24.9 (virtual t,[34] J_{CP} = 15.9, CH_2), 23.4 (s, CH_2); ^{31}P{^{1}H} 11.2 (s, J_{PPt} = 2488).[35]

IR (cm^{-1}, powder film) 2926 (m), 2860 (w), 1502 (s), 1459 (s), 1058 (s), 953 (s), 803 (s), 730 (s), 691 (s). MS:[29] 782 (**16a**$^+$, 40%), 746 ([**16a** − Cl]$^+$, 50%), 577 ([**16a** − Cl − C_6F_5]$^+$, 100%).

Metathesis of 11b

Complex **11b** (0.176 g, 0.198 mmol), **2** (0.039 g, 0.0474 mmol, 24 mol%), and CH_2Cl_2 (60 mL; resulting solution 0.0033 M in **11b**) were combined in a procedure analogous to that with **11a** (1.5 h, second catalyst charge, then 1.5 h). A similar workup (2.5 × 3 cm column) gave a white powder comprised of polymeric and/or oligomeric products (0.140 g, 0.168 mmol, 85%).

NMR:[27] ^{1}H 7.32 (m, 10 H, 2Ph), 5.30 (m, 4 H, 2CH=CH), 2.02–1.25 (m, 24 H, 12CH_2); ^{31}P{^{1}H} 10.0 (br s, J_{PPt} = 2561).[35]

MS:[29] 1632 ([2·**Pt** − Cl]$^+$, 30%),[36] 1463 ([2·**Pt** − Cl − C_6F_5]$^+$, 20%),[36] 630 (Pt(PPh((CH_2)$_3$CH=)$_2$)$_2^+$, 100%).

Metathesis of 11c; *syn*-(*E*,*E*)-*trans*-(Cl)(C_6F_5)-Pt(PPh(CH_2)$_4$CH=CH(CH_2)$_4$P(CH_2)$_4$CH=CH(CH_2)$_4$Ph) (*syn*-(*E*,*E*)-13c)

Complex **11c** (0.191 g, 0.202 mmol), **2** (0.020 g, 0.0242 mmol, 12 mol%), and CH_2Cl_2 (300 mL; resulting solution is 0.00067 M

in **11c**) were combined in a procedure analogous to that with **11a** (3 h, second catalyst charge, then 3 h; $^{31}P\{^1H\}$ NMR of residue (δ, $CDCl_3$): 18.7 (28%), 12.6 (11%), 12.0 (19%), 11.6 (23%), 11.1 (19%)) A similar workup (2.5 × 5 cm column using 2 : 1 v/v hexanes–CH_2Cl_2; solvent removal from first fractions) gave *syn*-(*E*,*E*)-**13c** as a white solid (0.0379 g, 0.0426 mmol, 21%), mp 265–268 °C (decomp.) (capillary). Calc. for $C_{38}H_{46}ClF_5P_2Pt$: C, 51.26; H, 5.17. Found: C, 51.12; H, 5.25%.

NMR:[27] ^1H 7.21 (m, 2 H of 2Ph), 7.13–7.10 (m, 8 H of 2Ph), 5.50 (t, J_{HH} = 3.6, 4 H, 2CH=CH), 2.53–2.45 (m, 8 H, $4CH_2$), 2.29–2.25 (m, 4 H, $2CH_2$), 2.09–2.07 (m, 4 H, $2CH_2$), 1.97–1.93 (m, 4 H, $2CH_2$), 1.82–1.79 (m, 4 H, $2CH_2$), 1.67–1.55 (m, 8 H, $4CH_2$); $^{13}C\{^1H\}$ [31,32] 131.5 (s, CH=CH), 130.7 (virtual t,[34] J_{CP} = 4.7, *o*-Ph), 130.0 (s, *p*-Ph), 128.0 (virtual t,[34] J_{CP} = 4.6, *m*-Ph), 32.2 (s, CH_2), 31.1 (virtual t,[34] J_{CP} = 8.3, CH_2), 27.4 (virtual t,[34] J_{CP} = 17.2, CH_2), 25.8 (s, CH_2); $^{31}P\{^1H\}$ 18.7 (s, J_{PPt} = 2623).[35]

IR (cm^{-1}, powder film) 2930 (m), 2849 (w), 1498 (s), 1455 (s), 1436 (s), 1058 (s), 953 (s), 768 (s), 718 (s). MS:[29] 890 (**13c**$^+$, 10%), 854 ([**13c** − Cl]$^+$, 100%), 686 ([**13c** − Cl − C_6F_5]$^+$, 60%).

The column was subsequently rinsed with CH_2Cl_2. Similar concentration of the fractions gave a white solid (0.0754 g, 0.0848 mmol, 42%) comprised of polymeric and/or oligomeric products.

$^{31}P\{^1H\}$ 12.6 (s, J_{PPt} = 2583,[35] 19%), 12.0 (s, J_{PPt} = 2552,[35] 14%), 11.6 (s, J_{PPt} = 2573,[35] 45%), 11.1 (s, J_{PPt} = 2498,[35] 22%).

MS:[29] 1742 ([2·**Pt** − Cl]$^+$, 10%),[36] 1576 ([2·**Pt** − Cl − C_6F_5]$^+$, 5%),[36] 549 ([**13c** − Cl − C_6F_5 − $(CH_2)_{10}$]$^+$, 100%).

syn-trans-(Cl)(C_6F_5)Pt(PPh$(CH_2)_{10}$P$(CH_2)_{10}$Ph) (*syn*-15c)

Complex **13c** (0.0379 g, 0.0426 mmol), 10% Pd/C (0.019 g, 0.018 mmol Pd), $ClCH_2CH_2Cl$ (10 mL), ethanol (10 mL), and H_2 were combined in a procedure analogous to that for **16a**. After 132 h, a similar workup (column rinsed with 2 : 1 v/v hexanes–CH_2Cl_2) gave *syn*-**15c** as a white powder (0.036 g, 0.0405 mmol, 95%), mp 256–258 °C (decomp.) (capillary), 255 °C (DSC; $T_i/T_e/T_p/T_c/T_f$ 210.1/242.2/254.6/260.6/271.4 °C). TGA: onset of mass loss, 328 °C (T_e). Calc. for $C_{38}H_{50}ClF_5P_2Pt$: C, 51.04; H, 5.60. Found: C, 51.00; H, 5.61%.

NMR:[27] ^1H 7.18 (m, 2 H of 2Ph), 7.11 (m, 8 H of 2Ph), 2.56–2.53 (m, 4 H, $2CH_2$), 2.42–2.35 (m, 4 H, $2CH_2$), 1.97–1.84 (m, 8 H, $4CH_2$), 1.70–1.63 (m, 10 H, $5CH_2$), 1.57–1.50 (m, 10 H, $5CH_2$), 1.48–1.40 (m, 4 H, $2CH_2$); $^{13}C\{^1H\}$ [31a,32] 130.9 (virtual t,[34] J_{CP} = 24.1, *i*-Ph), 130.7 (virtual t,[34] J_{CP} = 5.2, *o*-Ph), 130.0 (s, *p*-Ph), 127.9 (virtual t,[34] J_{CP} = 4.6, *m*-Ph), 29.5 (virtual t,[34] J_{CP} = 7.3, CH_2), 27.4 (s, CH_2), 26.6 (virtual t,[34] J_{CP} = 17.1, CH_2), 25.7 (s, CH_2), 24.8 (s, CH_2); $^{31}P\{^1H\}$ 16.2 (s, J_{PPt} = 2612).[35]

IR (cm^{-1}, oil film) 2926 (w), 2856 (w), 1502 (m), 1459 (m), 1231 (s), 1119 (s), 980 (s), 953 (s), 803 (m), 741 (m), 695 (m). MS:[29] 894 (**15c**$^+$, 35%), 858 ([**15c** − Cl]$^+$, 100%), 689 ([**15c** − Cl − C_6F_5]$^+$, 50%).

Metathesis of 11d; *syn-trans*-(Cl)(C_6F_5)Pt(PPh$(CH_2)_{12}$P$(CH_2)_{12}$Ph) (*syn*-15d)

Complex **11d** (0.103 g, 0.103 mmol), **2** (0.018 g, 0.0218 mmol, 21 mol%), and CH_2Cl_2 (55 mL; resulting solution 0.0019 M in **11d**) were combined in a procedure analogous to that with **11a** (2 h, second catalyst charge, 2 h). The residue ($^{31}P\{^1H\}$ NMR (δ, $CDCl_3$): 10.6 (s, 12%), 10.1 (br s, J_{PPt} = 2532.1, 88%))[35] was charged with 10% Pd/C (0.030 g, 0.028 mmol Pd), $ClCH_2CH_2Cl$ (10 mL) and ethanol (10 mL), flushed with H_2, and fitted with a balloon of H_2. The mixture was stirred for 144 h. Solvent was removed by oil-pump vacuum. The residue was filtered through neutral alumina (2.5 × 2.5 cm column) using 3 : 1 v/v hexanes–CH_2Cl_2. Solvent was removed from the filtrate to give *syn*-**15d** as a white powder (0.005 g, 0.0053 mmol, 5%). Calc. for $C_{42}H_{58}ClF_5P_2Pt$: C, 53.08; H, 6.11. Found: C, 53.34; H, 6.12%.

NMR:[27] ^1H 7.21–7.12 (m, 10 H, 2Ph), 2.53 (m, 4 H, $2CH_2$), 2.17 (m, 4 H, $2CH_2$), 1.95–1.80 (m, 8 H, $4CH_2$), 1.56–1.41 (m, 32 H, $16CH_2$); $^{13}C\{^1H\}$ [31,32] 130.9 (virtual t,[34] J_{CP} = 4.5, *o*-Ph), 130.0 (s, *p*-Ph), 127.9 (virtual t,[34] J_{CP} = 3.7, *m*-Ph), 30.2 (virtual t,[34] J_{CP} = 7.4, CH_2), 27.8 (s, CH_2), 27.3 (s, CH_2), 26.8 (virtual t,[34] J_{CP} = 17.2, CH_2), 26.5 (s, CH_2), 24.9 (s, CH_2); $^{31}P\{^1H\}$ 12.5 (s, J_{PPt} = 2590).[35]

MS:[29] 949 (**15d**$^+$, 30%), 913 ([**15d** − Cl]$^+$, 100%), 743 ([**15d** − Cl − C_6F_5]$^+$, 70%).

Metathesis of 11e; *trans*-(Cl)(C_6F_5)-Pt(PPh$(CH_2)_6$CH=CH$(CH_2)_6$P$(CH_2)_6$CH=CH$(CH_2)_6$Ph) (13e)

Complex **11e** (0.250 g, 0.236 mmol), **2** (0.0019 g, 0.0231 mmol, 10 mol%), and CH_2Cl_2 (70 mL; resulting solution 0.0034 M in **11e**) were combined in a procedure analogous to that with **11a** (2.5 h, second catalyst charge, 2.5 h). An identical workup gave **13e** and other metathesis products as a pale pink powder (0.230 g, 0.230 mmol, 97%). Calc. for $C_{46}H_{62}ClP_2F_5Pt$: C, 55.12; H, 6.23. Found: C, 54.91; H, 6.00%.

NMR:[27] ^1H 7.41–7.05 (m, 10 H, 2Ph), 5.35–5.20 (m, 4 H, 2CH=), 2.40–2.33 (m, 2 H of $4PCH_2$), 2.02–1.76 (m, 18 H; 6 H of $4PCH_2$, 4 H of $4PCH_2CH_2$, $4CH_2CH$=), 1.48–1.23 (m, 28 H; 4 H of $4PCH_2CH_2$, $12CH_2$); $^{31}P\{^1H\}$ (partial) 15.2 (s, 4%), 14.8 (s, 5%), 13.5 (s, $^1J_{PtP}$ = 2579,[35] 44%), 12.3 (s, 9%), 10.9 (s, 8%), 9.3 (s, 12%), 8.7 (s, 18%).

IR (cm^{-1}, powder film) 3057 (w), 2926 (w), 2853 (m), 1502 (m), 1459 (m), 1436 (m), 1104 (m), 1058 (m), 957 (s), 803 (m), 737 (s), 690 (s). MS:[29] 1969 ([2·**Pt** − Cl]$^+$, 30%),36 1798 ([2·**Pt** − Cl − C_6F_5]$^+$, 20%),[36] 966 ([**13e** − Cl]$^+$, 45%), 797 ([**13e** − Cl − C_6F_5]$^+$, 100%).

trans-(Cl)(C_6F_5)Pt(PPh$(CH_2)_{14}$P$(CH_2)_{14}$Ph) (15e)

Complex **13e** and other metathesis products (0.154 g, 0.153 mmol), 10% Pd/C (0.016 g, 0.015 mmol Pd), $ClCH_2CH_2Cl$ (6.5 mL), ethanol (6.5 mL), and H_2 were combined in a procedure analogous to that for **16a**. After 48 h, a similar workup (3 × 2.5 cm column rinsed with CH_2Cl_2) gave crude **15e** as a white powder (0.119 g, 0.118 mmol, 77%).

NMR:[27] ^1H 7.45–7.12 (m, 10 H, 2Ph), 2.40–2.36 (m, 4 H, $2PCH_2$), 2.15–2.14 (m, 4 H, $2PCH_2$), 1.88–1.87 (m, 4 H, $2PCH_2CH_2$), 1.77–1.75 (m, 4H, $2PCH_2CH_2$), 1.46–1.23 (m, 40 H, $20CH_2$); $^{31}P\{^1H\}$ (partial) 11.8 (s, $^1J_{PtP}$ = 2579,[35] **15e**, 52%).

MS:[29] 1977 ([2·**Pt** − Cl]$^+$, 20%),[36] 1809 ([2·**Pt** − Cl − C_6F_5]$^+$, 10%),[36] 1006 (**15e**$^+$, 40%), 970 ([**15e** − Cl]$^+$, 100%), 801 ([**15e** − Cl − C_6F_5]$^+$, 90%).

The sample was chromatographed on neutral alumina (10 × 2.5 cm column) using 1 : 3 v/v CH_2Cl_2–hexanes. The two least polar fractions were collected to give *syn*-**15e** (0.048 g, 0.0477 mmol, 31%) as a white powder, mp 155–157 °C, and *anti*-**15e** (0.011g, 0.0100 mmol, 7%) as a white powder.

syn-**15e**: Calc. for $C_{46}H_{66}ClP_2F_5Pt$: C, 54.89; H, 6.61. Found: C, 54.93; H, 6.75.

NMR:[27] ^1H [33b] 7.17–7.08 (m, 10 H, 2Ph), 2.35–2.28 (m, 4 H, 4PC*H*H′), 2.15–2.04 (m, 4 H, 4PCH*H*′), 1.82–1.80 (m, 4 H, $4PCH_2CHH'$), 1.73 (m, 4 H, $4PCH_2CHH'$), 1.47–1.11 (m, 40 H, $20CH_2$); $^{13}C\{^1H\}$ [31a,32,33] 130.3 (virtual t,[34] J_{CP} = 4.6, *o*-Ph), 130.2 (virtual t,[34] J_{CP} = 26.0, *i*-Ph), 129.5 (s, *p*-Ph), 127.6 (virtual t,[34] J_{CP} = 4.4, *m*-Ph), 30.4 (virtual t,[34] J_{CP} = 6.4, $PCH_2CH_2CH_2$), 27.9 (s, CH_2), 27.3 (s, CH_2), 27.0 (s, CH_2), 26.9 (s, CH_2), 24.2 (s and overlapping virtual t,[34] J_{CP} = 17.5, PCH_2CH_2 and PCH_2); $^{31}P\{^1H\}$ 11.8 (s, $^1J_{PtP}$ = 2560).[35]

IR (cm^{-1}, powder film) 2926 (m), 2856 (m), 1502 (s), 1463 (m), 1058 (m), 957 (s). MS:[29] 1006 (**15e**$^+$, 40%), 970 ([**15e** − Cl]$^+$, 100%), 801 ([**15e** − Cl − C_6F_5]$^+$, 60%).

anti-**15e**: Calc. for $C_{46}H_{66}ClP_2F_5Pt$: C, 54.89; H, 6.61. Found: C, 54.87; H, 6.91.

NMR:[27] ^1H 7.82–7.78 (m, 2H of 2Ph), 7.41–7.39 (4H of 2Ph), 7.30–7.10 (m, 4H of 2Ph), 2.30–2.26 (m, 2 H of 4PC*H*H′),[37] 2.14–2.05 (m, 2 H of 4PC*H*H′),[37] 1.87–1.82 (m, 4 H of 4PCH*H*′),[37] 1.62–1.10 (m, 48 H, $24CH_2$); $^{13}C\{^1H\}$ (partial,

some assignments tentative)[31a,37] 133.7 (s, *m*-Ph), 133.6 (s, *m*-Ph′), 130.4 (br s, 2 *p*-Ph), 129.60 (s, *i*-Ph), 129.58 (s, *i*-Ph′), 127.8 (virtual t,[34] J_{CP} = 8.5, *o*-Ph), 127.99 (virtual t,[34] J_{CP} = 8.5, *o*-Pp′), 30.06 (virtual t,[34] J_{CP} = 11.5, CH_2), 30.04 (virtual t,[34] J_{CP} = 11.5, CH_2), 28.2 (s, CH_2), 28.0 (s, CH_2), 27.7 (br s, CH_2), 27.4 (br s, CH_2), 27.1 (br s, CH_2), 26.9 (br s, CH_2), 24.2 (br s, CH_2), 23.7 (br s, CH_2); $^{31}P\{^1H\}$ 15.8 ($^2J_{PP'}$ = 426.8, $^1J_{PPt}$ = 2610),[35] 11.2 ($^2J_{P'P}$ = 426.8, $^1J_{P'Pt}$ = 2556).[35]

IR (cm^{-1}, powder film) 2926 (s), 2856 (s), 2362 (w), 2335 (w), 1502 (s), 1459 (m), 1440 (s), 1061 (s), 957 (s). MS:[29] 1006 (**15e**$^+$, 20%), 971 ([**15e** − Cl]$^+$, 90%), 799 ([**15e** − Cl − C_6F_5]$^+$, 100%).

Metathesis of 11f: *trans*-(Cl)(C_6F_5)-Pt(PPh(CH_2)$_8$CH=CH(CH_2)$_8$P(CH_2)$_8$CH=CH(CH_2)$_8$Ph) (13f)

Complex **11f** (0.273 g, 0.233 mmol), **2** (ca. half of 0.050 g, 0.0608 mmol, 26 mol%), and CH_2Cl_2 (70 mL; resulting solution 0.0033 M in **11f**) were combined in a procedure analogous to that with **11a** (2 h, second catalyst charge, 3.5 h). A similar workup (2.5 × 3 cm column) gave **13f** and other metathesis products as a pale pink solid (0.238 g, 0.214 mmol, 92%). Calc. for $C_{54}H_{78}ClF_5P_2Pt$: C, 58.20; H, 6.88. Found: C, 57.84; H, 7.30%.

NMR:[27] ^1H 7.44–7.14 (m, 10 H, 2Ph), 5.36 (m, 4 H, 2CH=CH), 2.27–1.86 (m, 16 H, 8CH_2), 1.46–1.11 (m, 48 H, 24CH_2); $^{31}P\{^1H\}$ 13.5 (s, 7%), 13.1 (s, J_{PPt} = 2566,[35] 34%), 12.6 (11%), 10.7 (s, J_{PPt} = 2522,[35] 23%), 10.5 (s, J_{PPt} = 2522, 25%).[35]

MS:[29] 1079 ([**13f** − Cl]$^+$, 100%), 909 ([**13f** − Cl − C_6F_5]$^+$, 80%).

syn-trans-(Cl)(C_6F_5)Pt(PPh(CH_2)$_{18}$P(CH_2)$_{18}$Ph) (*syn*-15f)

Complex **13f** and other metathesis products (0.171 g, 0.154 mmol), 10% Pd/C (0.027 g, 0.0262 mmol Pd), $ClCH_2CH_2Cl$ (10 mL), ethanol (10 mL), and H_2 were combined in a procedure analogous to that for **16a**. After 71 h, a similar workup ($^{31}P\{^1H\}$ NMR of residue (δ, $CDCl_3$): 11.9 (8%), 10.8 (39%), 10.3 (27%), 10.1 (21%), 8.7 (5%); 2.5 × 5 cm column) gave *syn*-**15f** as a colorless oil (0.026 g, 0.023 mmol, 15%).[30]

NMR:[27] ^1H 7.50–7.10 (m, 10 H, 2Ph), 2.15 (m, 10 H, 5CH_2), 1.35 (m, 62 H, 31CH_2); $^{13}C\{^1H\}$ [31a,32] 131.4 (virtual t,[34] J_{CP} = 4.9, *o*-Ph), 130.8 (virtual t,[34] J_{CP} = 26.0, *i*-Ph), 130.1 (s, *p*-Ph), 128.3 (virtual t,[34] J_{CP} = 4.8, *m*-Ph), 31.0 (virtual t,[34] J_{CP} = 6.8, CH_2), 28.9, 28.8, 28.7, 28.6, 28.5, 28.4, 24.1 (s, CH_2), 23.6 (virtual t,[34] J_{CP} = 17.2, CH_2); $^{31}P\{^1H\}$ 10.8 (s, J_{PPt} = 2551).[35]

MS:[29] 1081 ([**15f** − Cl]$^+$, 100%), 913 ([**15f** − Cl − C_6F_5]$^+$, 90%).

$H_3B{\cdot}PPh((CH_2)_6CH{=}CH_2)_2$ (17e)

A Schlenk flask was charged with **4e** (0.304g, 0.920 mmol)[3c] and THF (2 mL), cooled to −20 °C (N_2, acetone), and $H_3B{\cdot}SMe_2$ (0.0698g, 0.920 mmol) was added. The solution was stirred for 1 h at −20 °C and 30 min at room temperature. Solvent was removed by rotary evaporation and oil-pump vacuum. The residue was filtered through neutral alumina (6 × 2.5 cm column) using 1 : 1 v/v CH_2Cl_2–hexanes. Solvent was removed from the product fraction by oil-pump vacuum to give **17e** as a colorless oil (0.205 g, 0.595 mmol, 65%). Calc. for $C_{22}H_{38}BP$: C, 76.74; H, 11.12. Found: C, 76.46; H, 11.39%.

NMR:[27] ^1H 7.73–7.70 (m, 2 H of Ph), 7.60–7.47 (m, 3 H of Ph), 5.82–5.76 (m, 2 H, 2CH=), 5.01–4.92 (m, 4 H, 2 =CH_2), 2.02–1.99 (m, 4 H, 2CH_2CH=), 1.87–1.81 (m, 4 H, 2PCH_2), 1.57 (m, 2 H, CH_2), 1.37–1.26 (m, 14 H, 7CH_2), 1.0–0.2 (br, 3 H, BH_3); $^{13}C\{^1H\}$ [28] 138.6 (s, CH=), 131.8 (d, J_{CP} = 7.6, *o*-Ph), 131.1 (d, J_{CP} = 2.2, *p*-Ph) 128.7 (d, J_{CP} = 9.5, *m*-Ph), 128.6 (d, $^1J_{CP}$ = 51.3, *i*-Ph), 114.5 (s, =CH_2), 33.6 (s, CH_2CH=), 30.9 (d, J_{CP} = 13.0, CH_2), 28.6 (s, CH_2), 28.5 (s, CH_2), 25.6 (d, J_{CP} = 36.0, CH_2), 22.7 (s, CH_2); $^{31}P\{^1H\}$ 15.3 (apparent d, $^1J(^{11}B,^{31}P)$ = 75.1).

IR (cm^{-1}, oil film) 2930, 2856, 2374, 2339, 1640, 1463, 1436, 1116, 1061, 996, 907, 799, 745, 695. MS:[29] 341 ([**17e** − 3H]$^+$,[38] 40%), 331 ([**17e** − H_3B]$^+$, 100%).

$H_3B{\cdot}PPh(CH_2)_6CH{=}CH(CH_2)_6$ (18e)

A two-necked flask was charged with **17e** (0.141 g, 0.409 mmol), **2** (*ca.* half of 0.017 g, 0.0205 mmol, 5 mol%), and CH_2Cl_2 (180 mL, the resulting solution is 0.0023 M in **17e**), and fitted with a condenser. The solution was refluxed. After 2.5 h, the remaining **2** was added. After 2.5 h, solvent was removed by rotary evaporation and oil-pump vacuum. The residue was filtered through neutral alumina (5 × 2.5 cm column) using CH_2Cl_2. Solvent was removed from the filtrate by rotary evaporation and oil-pump vacuum to give **18e** as a pale pink oil (0.080 g, 0.253 mmol, 62%). Calc. for $C_{20}H_{34}BP$: C, 75.95; H, 10.83. Found: C, 75.20; H, 11.25%.

NMR:[27] ^1H 7.72–7.70 (m, 2 H of Ph), 7.49–7.46 (m, 3 H of Ph), 5.47–5.43/5.42–5.39/5.38–5.33 (3m, 2 H, 2CH=), 2.13–1.82 (m, 8 H, 2CH_2CH=, 2PCH_2), 1.57–1.27 (m, 16 H, 8CH_2), 1.0–0.3 (br, 3H, BH_3); $^{31}P\{^1H\}$ 15.2 (m).

IR (cm^{-1}, oil film) 2926, 2853, 2370, 2339, 1436, 1112, 1061, 969, 741, 695. MS:[29] 629 ([2·**P**]$^+$, 20%),[36] 617 ([2·**P** − H_3B]$^+$, 25%),[36] 605 ([2·**P** − 2H_3B]$^+$, 30%),[36] 315 (**18e**$^+$, 80%), 303 ([**18e** − H_3B]$^+$, 100%).

$H_3B{\cdot}PPh(CH_2)_{14}$ (19e)

A Fischer–Porter bottle was charged with **18e** (0.072 g, 0.228 mmol), $Rh(PPh_3)_3(Cl)$ (0.021 g, 0.0028 mmol, 10 mol%), and benzene (25 mL), and flushed with H_2. The mixture was stirred under H_2 (6 atm) for 20 h. Solvent was removed by oil-pump vacuum. The residue was chromatographed on neutral alumina (10 × 2.5 cm column) using 1 : 1 v/v CH_2Cl_2–hexanes. Solvent was removed from the product fraction by oil-pump vacuum to give **19e** as a colorless oil (0.056 g, 0.176 mmol, 77%). Calc. for $C_{20}H_{36}BP$: C, 75.74; H, 11.40. Found: C, 75.28; H, 11.54%.

NMR:[27] ^1H 7.73–7.70 (m, 2 H of Ph), 7.49–7.46 (m, 3 H of Ph), 2.00–1.84 (m, 4 H, 2PCH_2), 1.57–1.21 (m, 24 H, 12CH_2), 1.1–0.3 (br, 3H, BH_3); $^{13}C\{^1H\}$ [28] 131.3 (d, J_{CP} = 8.2, *o*-Ph), 130.9 (d, J_{CP} = 2.3, *p*-Ph) 130.2 (d, $^1J_{CP}$ = 53.1, *i*-Ph), 128.7 (d, J_{CP} = 9.5, *m*-Ph), 28.9 (d, J_{CP} = 11.5, CH_2), 26.8 (s, CH_2), 26.57 (s, CH_2), 26.54 (s, CH_2), 26.3 (s, CH_2), 23.8 (d, J_{CP} = 34.5, CH_2), 21.5 (d, J_{CP} = 2.4, CH_2); $^{31}P\{^1H\}$ 15.4 (apparent d, $^1J(^{11}B,^{31}P)$ = 69.6).

IR (cm^{-1}, oil film) 2926, 2853, 2374, 2343, 1459, 1435, 1112, 1065, 1000, 737, 691. MS:[29] 609 ([2·**P** − 2H_3B]$^+$, 30%),[36] 315 ([**19e** − 3H]$^+$, 100%),[38] 305 ([**19e** − H_3B]$^+$, 60%).

trans-(Cl)(C_6F_5)Pt(PPh(CH_2)$_{14}$)$_2$ (16e)

A Schlenk flask was charged with **19e** (0.112 g, 0.352 mmol) and $HNEt_2$ (2 mL). The mixture was heated to 50 °C and stirred for 45 min. The $HNEt_2$ was removed by oil-pump vacuum, and the residue vacuum dried at 50 °C for an additional 20 min. This operation was repeated twice (final cycle: 2 h, 50 °C) to give crude PPh(CH_2)$_{14}$ (**20e**). The flask was charged with **12** (0.085 g, 0.088 mmol)[9] and CH_2Cl_2 (6 mL), and the mixture was stirred (16 h). Solvent was removed by oil-pump vacuum. The residue was chromatographed on neutral alumina (9 × 2.5 cm column) using 1 : 1 v/v CH_2Cl_2–hexanes. Solvent was removed from the product fraction by oil-pump vacuum to yield **16e** as a colorless oil, which solidified over the course of several days (0.042 g, 0.0417 mmol, 24% based on **19e**). Calc. for $C_{46}H_{66}ClF_5P_2Pt$: C, 54.89; H, 6.61. Found: C, 54.71; H, 6.55%.

NMR:[27] ^1H 7.50–7.45 (m, 4 H of 2Ph), 7.36–7.28 (m, 6 H of 2Ph), 2.16–2.12 (m, 4 H of 4PCHH′),[37] 1.95–1.92 (m, 4 H of 4PCHH′),[37] 1.65–1.63 (m, 4 H of 4PCH_2CHH'),[37] 1.56–1.30 (m, 44 H; 4 H of 4PCH_2CHH', 20CH_2);[37] $^{13}C\{^1H\}$ [31a,32,33] 131.2

(virtual t,[34] J_{CP} = 5.2, *o*-Ph), 130.9 (virtual t,[34] J_{CP} = 25.8, *i*-Ph), 129.8 (s, *p*-Ph), 128.1 (virtual t,[34] J_{CP} = 4.7, *m*-Ph), 28.9 (virtual t,[34] J_{CP} = 6.6, $PCH_2CH_2CH_2$), 26.8 (s, CH_2), 26.63 (s, CH_2), 26.59 (s, CH_2), 26.3 (s, CH_2), 21.8 (s, CH_2), 21.2 (virtual t,[34] J_{CP} = 16.6, PCH_2); $^{31}P\{^1H\}$ 7.2 (s, $^1J_{PPt}$ = 2520).[35]

IR (cm^{-1}, powder film) 2926, 2856, 2374, 1502, 1455, 1112, 1061, 957, 803, 745, 695. MS:[29] 1006 (**16e**$^+$, 15%), 970 ([**16e** − Cl]$^+$, 40%), 801 ([**16e** − Cl − C_6F_5]$^+$, 60%)]$^+$, 495 ([**16e** − Cl − C_6F_5 − **20e**]$^+$, 90%), 305 (**20e**$^+$, 100%).

Crystallography.[15]

Toluene solutions of *syn*-**15e**, *anti*-**15e** and **16e** were layered with ethanol. The samples were stored at −20 °C. After three to thirty days, colorless prisms had formed. Complexes **16a**, *syn*-(*E,E*)-**13c**, and *syn*-**15c** were suspended in methanol and warmed. THF was added until the samples were homogeneous. The mixtures were kept at room temperature. After one day, colorless prisms had formed.

Data were collected as outlined in Table 1. Cell parameters were obtained from 10 frames using a 10° scan and refined with ≥6873 reflections (*syn*-**15e**, 10003; *anti*-**15e**, 7885; **16e**, 9914; **16a**, 6873; *syn*-(*E,E*)-**13c**, 8701; *syn*-**15c**, 23439). Lorentz, polarization, and absorption corrections were applied.[39] The space groups were determined from systematic absences and subsequent least-squares refinement. The structures were solved by direct methods. The parameters were refined with all data by full-matrix-least-squares on F^2 using SHELXL-97.[40] Non-hydrogen atoms were refined with anisotropic thermal parameters. The hydrogen atoms were fixed in idealized positions using a riding model. Scattering factors were taken from literature.[41] The quality of the crystal of *syn*-**15c**, which contained two independent molecules in the unit cell, was lower than the others.

CCDC reference numbers: *syn*-**15e**, 159809; *anti*-**15e**, 227266; **16e**, 227267; **16a**, 227269; *syn*-(*E,E*)-**13c**, 227270; *syn*-**15c**, 227268.

See http://www.rsc.org/suppdata/dt/b4/b400156g/ for crystallographic data in CIF or other electronic format.

Acknowledgements

We thank the Deutsche Forschungsgemeinschaft (DFG, GL 300/1–3), Alexander von Humboldt Foundation (Fellowship to T. S.), and Johnson Matthey PMC (platinum and ruthenium loans) for support.

References

1 E. B. Bauer and J. A. Gladysz, in *Handbook of Metathesis*, ed. R. H. Grubbs, Wiley-VCH, Weinheim, Germany, 2003, vol. 2, pp 395–423.
2 (*a*) M. Weck, B. Mohr, J.-P. Sauvage and R. H. Grubbs, *J. Org. Chem.*, 1999, **64**, 5463; (*b*) C. Dietrich-Buchecker, G. Rapenne and J.-P. Sauvage, *Chem. Commun.*, 1997, 2053; (*c*) C. Dietrich-Buchecker and J.-P. Sauvage, *Chem. Commun.*, 1999, 615; (*d*) G. Rapenne, C. Dietrich-Buchecker and J.-P. Sauvage, *J. Am. Chem. Soc.*, 1999, **121**, 994; (*e*) N. Belfrekh, C. Dietrich-Buchecker and J.-P. Sauvage, *Inorg. Chem.*, 2000, **39**, 5169; (*f*) P. Mobian, J.-M. Kern and J.-P. Sauvage, *J. Am. Chem. Soc.*, 2003, **125**, 2016; (*g*) P. Mobian, J.-M. Kern and J.-P. Sauvage, *Helv. Chim. Acta.*, 2003, **86**, 4195; (*h*) P. Mobian, J.-M. Kern and J.-P. Sauvage, *Inorg. Chem.*, 2003, **42**, 8633.
3 (*a*) J. M. Martín-Alvarez, F. A. Hampel, A. M. Arif and J. A. Gladysz, *Organometallics*, 1999, **18**, 955; (*b*) E. B. Bauer, J. Ruwwe, J. M. Martín-Alvarez, T. B. Peters, J. C. Bohling, F. A. Hampel, S. Szafert, T. Lis and J. A. Gladysz, *Chem. Commun.*, 2000, 2261; (*c*) J. Ruwwe, J. M. Martín-Alvarez, C. R. Horn, E. B. Bauer, S. Szafert, T. Lis, F. Hampel, P. C. Cagle and J. A. Gladysz, *Chem. Eur. J.*, 2001, **7**, 3931; (*d*) E. B. Bauer, F. Hampel and J. A. Gladysz, *Organometallics*, 2003, **22**, 5567.
4 (*a*) J. Stahl, J. C. Bohling, E. B. Bauer, T. B. Peters, W. Mohr, J. M. Martín-Alvarez, F. Hampel and J. A. Gladysz, *Angew. Chem.*, 2002, **114**, 1951; J. Stahl, J. C. Bohling, E. B. Bauer, T. B. Peters, W. Mohr, J. M. Martín-Alvarez, F. Hampel and J. A. Gladysz, *Angew. Chem., Int. Ed.*, 2002, **41**, 1872; (*b*) C. R. Horn, J. M. Martín-Alvarez and J. A. Gladysz, *Organometallics*, 2002, **21**, 5386.
5 (*a*) A. V. Chuchuryukin, H. P. Dijkstra, B. M. J. M. Suijkerbuijk, R. J. M. Klein Gebbink, G. P. M. van Klink, A. M. Mills, A. L. Spek and G. van Koten, *Angew. Chem.*, 2003, **115**, 238; A. V. Chuchuryukin, H. P. Dijkstra, B. M. J. M. Suijkerbuijk, R. J. M. Klein Gebbink, G. P. M. van Klink, A. M. Mills, A. L. Spek and G. van Koten, *Angew. Chem., Int. Ed.*, 2003, **42**, 228; (*b*) V. Martinez, J.-C. Blais and D. Astruc, *Angew. Chem.*, 2003, **115**, 4502; V. Martinez, J.-C. Blais and D. Astruc, *Angew. Chem., Int. Ed.*, 2003, **42**, 4366; (*c*) T. Inomata and K. Konishi, *Chem. Commun.*, 2003, 1282.
6 C. A. Bessel, P. Aggarwal, A. C. Marschilok and K. J. Takeuchi, *Chem. Rev.*, 2001, **101**, 1031.
7 (*a*) P. E. Garrou and G. E. Hartwell, *J. Organomet. Chem.*, 1974, **71**, 443; (*b*) P. W. Clark, P. Hanisch and A. J. Jones, *Inorg. Chem.*, 1979, **18**, 2067.
8 M. A. Bennett, H. W. Kouwenhoven, J. Lewis and R. S. Nyholm, *J. Chem. Soc.*, 1964, 4570.
9 R. Usón, J. Forniés, P. Espinet and G. Alfranca, *Synth. React. Inorg. Met.-Org., Chem.*, 1980, **10**, 579.
10 R. Usón, J. Forniés, P. Espinet, R. Navarro and C. Fortuño, *J. Chem. Soc., Dalton Trans.*, 1987, 2077.
11 W. Mohr, J. Stahl, F. Hampel and J. A. Gladysz, *Chem. Eur. J.*, 2003, **9**, 3324.
12 (*a*) M. Schuman, M. Trevitt, A. Redd and V. Gouverneur, *Angew. Chem.*, 2000, **112**, 2604; M. Schuman, M. Trevitt, A. Redd and V. Gouverneur, *Angew. Chem., Int. Ed.*, 2000, **39**, 2491; (*b*) C. A. Slinn, A. J. Redgrave, S. L. Hind, C. Edlin, S. P. Nolan and V. Gouverneur, *Org. Biomol. Chem.*, 2003, **1**, 3820.
13 M. Leconte, I. Jourdan, S. Pagano, F. Lefebvre and J.-M. Basset, *J. Chem. Soc., Chem. Commun.*, 1995, 857.
14 T. Imamoto, T. Kusumoto, N. Suzuki and K. Sato, *J. Am. Chem. Soc.*, 1985, **107**, 5301.
15 The atom numbering in Tables 2 and 3, and Figs. 1–3, 5, and 6, has been altered from those in the CIF files to facilitate comparisons between molecules.
16 (*a*) J. C. Collings, K. P. Roscoe, E. G. Robins, A. S. Batsanov, L. M. Stimson, J. A. K. Howard, S. J. Clark and T. B. Marder, *New J. Chem.*, 2002, **26**, 1740, and references therein.; (*b*) F. Ponzini, R. Zagha, K. Hardcastle and J. S. Siegel, *Angew. Chem.*, 2000, **112**, 2413; F. Ponzini, R. Zagha, K. Hardcastle and J. S. Siegel, *Angew. Chem., Int. Ed.*, 2000, **39**, 2323; (*c*) G. W. Coates, A. R. Dunn, L. M. Henling, J. W. Ziller, E. B. Lobkovsky and R. H. Grubbs, *J. Am. Chem. Soc.*, 1998, **120**, 3641; (*d*) M. L. Renak, G. P. Bartholomew, S. Wang, P. J. Ricatto, R. J. Lachicotte and G. C. Bazan, *J. Am. Chem. Soc.*, 1999, **121**, 7787.
17 J. Sandström, *Dynamic NMR Spectroscopy*, Academic Press, New York, 1982; calculations utilized eqn. 7.4c.
18 (*a*) B. L. Shaw, *J. Am. Chem. Soc.*, 1975, **97**, 3856; (*b*) A. Pryde, B. L. Shaw and B. Weeks, *J. Chem. Soc., Dalton. Trans.*, 1976, 322.
19 While this paper was being reviewed, we found that *syn*-(*E,E*)-**13c** could be isolated in up to 58% yield using Grubbs' "second generation" catalyst Ru(=CHPh)(H_2IMes)(PCy_3)($Cl)_2$ (20 mol%) and extended reaction times that partially transform the byproducts. Analogous enhancements were not observed with **11d**,**f**, nor with the metatheses in Scheme 1.[3d] These results will described, together with data for other advanced-generation catalysts, at a later date.
20 P. L. Ng and J. N. Lambert, *Synlett*, 1999, 1749.
21 (*a*) P. G. Sammes and D. J. Weller, *Synthesis*, 1995, 1205; (*b*) M. D. E. Forbes, J. T. Patton, T. L. Myers, H. D. Maynard, D. W. Smith, Jr., G. R. Schulz and K. B. Wagener, *J. Am. Chem. Soc.*, 1992, **114**, 10978.
22 E. B. Bauer, S. Szafert, F. Hampel and J. A. Gladysz, *Organometallics*, 2003, **22**, 2184.
23 E. B. Bauer, Doctoral Dissertation, Universität Erlangen-Nürnberg, 2003.
24 A. Bondi, *J. Phys. Chem.*, 1964, **68**, 441.
25 T. Shima, F. Hampel, J. A. Gladysz, manuscript in preparation.
26 H. K. Cammenga and M. Epple, *Angew. Chem.*, 1995, **107**, 1284; H. K. Cammenga and M. Epple, *Angew. Chem., Int. Ed.*, 1995, **34**, 1171.
27 δ, $CDCl_3$; all *J* values are in Hz.
28 The PC_6H_5 ^{13}C NMR signals were assigned as described by B. E. Mann, *J. Chem. Soc., Perkin Trans. 2*, 1972, 30; that with the chemical shift closest to benzene was attributed to the *meta* carbon, and the least intense phosphorus-coupled signal was attributed to the *ipso*, carbon.

29 FAB, 3-NBA, *m*/*z*, (relative intensity, %); the most intense peak of isotope envelope is given.
30 A satisfactory microanalysis was not obtained.
31 (*a*) The C_6F_5 ^{13}C NMR signals were not observed. These require larger numbers of transients due to the fluorine and platinum couplings; (*b*) The *ipso* PC_6H_5 ^{13}C NMR signals were not observed.
32 The $PtPC_6H_5$ ^{13}C NMR assignments have abundant precedent. See, for example: P. W. Jolly and R. Mynott, *Adv. Organomet. Chem.*, 1981, **19**, 257.
33 (*a*) For *syn*-**15e**, the $PtPCH_2CH_2CH_2$ ^{13}C assignments were confirmed by a ^1H,^{13}C COSY spectrum. The corresponding signals in **11b**–**f** and **16e**, and the $PtPCH_2CH_2CH$= signals of **11a**, were assigned by analogy; (*b*) The ^1H assignments for *syn*-**15e** were in turn verified by a ^1H,^1H COSY experiment.
34 P. S. Pregosin and L. M. Venanzi, *Chem. Br.*, 1978, 276; the *apparent*, coupling between adjacent peaks of the triplet is given.
35 This coupling represents a satellite (d; ^{195}Pt = 33.8%), and is not reflected in the peak multiplicity given.
36 The abbreviations 2·**Pt** and 2·**P** indicate ions with twice the mass of the expected monoplatinum or monophosphorus products.
37 The PCH_2CH_2 ^1H and C_6H_5 ^{13}C NMR signals were assigned by analogy to *syn*-**15e**.
38 The isotope envelope calculated for this ion agreed with that observed. For phosphine boranes that give analogous ions, see ref. 12*a*.
39 (*a*) "Collect" data collection software, Nonius B.V., Delft, 1998; (*b*) "Scalepack" data processing software Z. Otwinowski and W. Minor, *Methods Enzymol. A*, 1997, **276**, 307.
40 G. M. Sheldrick, SHELX-97, Program for refinement of crystal structures, University of Göttingen, 1997.
41 D. T. Cromer and J. T. Waber, in *International Tables for X-ray Crystallography*, ed. J. A. Ibers and W. C. Hamilton, Kynoch Press, Birmingham, England, 1974.